JOURNAL OF THE ROYAL SOCIETY Interface

J. R. Soc. Interface (2010) **7**, 3–18
doi:10.1098/rsif.2009.0243
Published online 16 September 2009

REVIEW

Optical imaging-guided cancer therapy with fluorescent nanoparticles

Shan Jiang[1], Muthu Kumara Gnanasammandhan[1] and Yong Zhang[1,2,*]

[1]*Division of Bioengineering, Faculty of Engineering, and* [2]*Nanoscience and Nanotechnology Initiative, National University of Singapore, Singapore 117576, Republic of Singapore*

The diagnosis and treatment of cancer have been greatly improved with the recent developments in nanotechnology. One of the promising nanoscale tools for cancer diagnosis is fluorescent nanoparticles (NPs), such as organic dye-doped NPs, quantum dots and upconversion NPs that enable highly sensitive optical imaging of cancer at cellular and animal level. Furthermore, the emerging development of novel multi-functional NPs, which can be conjugated with several functional molecules simultaneously including targeting moieties, therapeutic agents and imaging probes, provides new potentials for clinical therapies and diagnostics and undoubtedly will play a critical role in cancer therapy. In this article, we review the types and characteristics of fluorescent NPs, *in vitro* and *in vivo* imaging of cancer using fluorescent NPs and multi-functional NPs for imaging-guided cancer therapy.

Keywords: fluorescent nanoparticles; cancer therapy; optical imaging

1. INTRODUCTION

Cancer is one of the major causes of mortality and morbidity in the world and the incidence of cancer continues to increase. The common cancer treatment methods include surgery, chemotherapy and radiation therapy; however, current therapies are limited by ineffective early diagnosis, insufficient drug concentrations reaching the tumour, systemic toxicity, adverse effects of drugs and lack of capability to monitor therapeutic responses. Thus, the important issues in improving treatment regimens are (i) development of advanced imaging technologies for early diagnosis and to track therapeutic responses; (ii) utilization of targeting moieties to specifically and efficiently deliver drugs to tumour tissues; and (iii) discovery in cancer biology and genetics leading to new knowledge for cancer treatment.

Nanotechnology is a new field of interdisciplinary research to fabricate materials with nanoscale dimensions between 1 and 1000 nm (Ferrari 2005). Materials at the nanometre scale have novel optical, electronic, magnetic and structural properties compared with the same materials at bulk volume, making them attractive for use in cancer diagnosis and therapy. Recent research has developed a number of nanoparticles (NPs), such as metal, semiconductor and polymeric particles, to be used as imaging probes, delivery vehicles, and even as multi-functional NPs (Liu *et al.* 2007*a*; Wang *et al.* 2008; Riehemann *et al.* 2009). NP-based drug-delivery systems based on chitosan, polyethyleneimine (PEI), liposomes, micelles and silica NPs offer the potential to optimize drug delivery while reducing drug side effects (Sinha *et al.* 2006; Cho *et al.* 2008). There are also several types of NPs used in optical molecular imaging in cancer diagnosis, such as organic dye-doped polymer and liposomes, quantum dots (QDs) and upconversion NPs (UCNs; Licha & Olbrich 2005; Santra *et al.*, 2005; Grodzinski *et al.* 2006; Rao *et al.* 2007). More importantly, NPs are capable of combining different modalities (targeting, imaging, drug delivery and sensing) on one particle, which leads to multi-functional NPs for simultaneous tumour imaging and treatment (Torchilin 2006; Sanvicens & Marco 2008; Suh *et al.* 2009). With the engineered multi-functional NPs, imaging-guided cancer therapy can be realized.

In this article, we review the types and characteristics of fluorescent NPs, *in vitro* and *in vivo* imaging of cancer using fluorescent NPs and multi-functional NPs for simultaneous tumour imaging and treatment.

2. FLUORESCENT NANOPARTICLES

Optical imaging is the latest trend in imaging-guided therapy that involves the detection of light photons transmitted through tissues. It can non-invasively monitor the progression of disease and therapy. Conventional fluorophores such as fluorescent dyes, bioluminescent proteins and fluorescent proteins were used initially. But the recent advancements in the development of fluorescent NPs have made them potential candidates for imaging-guided therapy and they have a lot of advantages over their predecessors.

*Author for correspondence (biezy@nus.edu.sg).

Received 21 June 2009
Accepted 17 August 2009

2.1. Organic dye-doped nanoparticles

Recently, there has been a surge in the development of NPs doped with organic dyes for imaging. Nanoencapsulation of the organic dyes makes them more stable and amplifies the signal considerably. The NPs are usually made of silica, but sometimes other polymers like poly(D,L-lactic-co-glycolic acid) (PLGA; Suzuki *et al.* 2008) are also used. These NPs have been doped with many organic dyes like IRG-023 Cy5, fluorescein isothiocyanate (FITC), rhodamine B isothiocyanate (RITC), etc. (Liu *et al.* 2006; He *et al.* 2007; Shi *et al.* 2007*b*; Suzuki *et al.* 2008). Labelling of NPs with a combination of dyes has also been reported (Wang *et al.* 2005*a*; Gao *et al.* 2007).

The organic dye-doped NPs are usually synthesized by two main methods namely the Stober method and the microemulsion method. The size varies from 2 to 200 nm and can be controlled. The NPs produce light of high intensity due to the large number of dye molecules within each particle and they are quite photostable. The photostability is mainly due to the polymer coating that prevents the penetration of oxygen, thereby reducing the bleaching (Zhou & Zhou 2004). Many of these NPs exhibit good biocompatibility and water solubility and universal bioconjugation strategies can be used for attaching biomolecules to them. The versatile silica chemistry is used for bioconjugation through functional groups such as thiol, amino and carboxyl groups. Interactions between avidin and biotin are also employed (Tapec *et al.* 2002).

2.2. Quantum dots

QDs are semiconductor crystals with sizes in the nanometre range. They are composed of elements from groups II to VI, III to IV or IV to VI from the periodic table. The size of the QD is usually from 2 to 10 nm, which gives them special properties not seen at a macro-level owing to the effect of quantum confinement. QDs have a broad absorption spectrum, i.e. they can be excited by a wide range of wavelengths and they have a narrow emission spectrum. They also have extensive tunability whereby the emission wavelength can be controlled by the size of the QDs. Multi-coloured QDs that can be excited by a single wavelength are very useful in cellular imaging with multiple labels.

QDs are usually synthesized by heating the precursors dissolved in organic solvents at high temperatures of about 300°C (Dabbousi *et al.* 1997; Talapin *et al.* 2001; Reiss *et al.* 2002; Bang *et al.* 2008). The size of the QDs can be varied by varying the concentration of the precursors and the crystal growth time. The nanocrystals thus formed have a hydrophobic core and are thus insoluble in water. So various surface modifications such as silica encapsulation, ligand exchange, conjugation to mercaptohydrocarbonic acids, dithiothretol and oligomeric ligands are carried out to make them soluble in water, which is essential for biological applications (Gerion *et al.* 2001; Pathak *et al.* 2001; Kim & Bawendi 2003; Nann & Mulvaney 2004). Conjugation of biomolecules on the surface of the QDs is usually by physical adsorption and electrostatic interactions (Lakowicz *et al.* 2000; Mattoussi *et al.* 2000; Jaiswal *et al.* 2003) but covalent coupling with linkers (Goldman *et al.* 2001; Winter *et al.* 2001; Parak *et al.* 2002) is also used routinely.

QDs are very bright, photostable and thermostable. They are quite resistant to photobleaching and can be used for *in vivo* tracking for extended periods of time. Toxicity of these QDs has always been in question and cytotoxic studies of CdTe and CdSe QDs were reported (Shiohara *et al.* 2004; Lovric *et al.* 2005). However, the cytotoxicity is dependent on the dose, mode of particle preparation, surface coating, etc. The coating of the particles with hydrophilic polymers and ZnS prevents the leaching of the toxic elements such as cadmium and selenium, thereby reducing the toxicity considerably. Thus, QDs are more stable for long times in *in vivo* imaging than the dye-doped NPs and have been used widely (Dubertret *et al.* 2002; Gao *et al.* 2004; Jaiswal *et al.* 2004).

To overcome the problems of using UV light as the excitation source for the visible QDs, near-infrared (NIR) QDs were developed, which can be excited by NIR light (Iyer *et al.* 2006; Yong 2009). The use of UV light as a source causes damage to biological components, generates singlet oxygen, has low penetration depths, high background autofluorescence, etc. Thus, NIR QDs overcome all these problems and are more efficient and suitable for *in vivo* and real time fluorescence imaging.

2.3. Upconversion nanoparticles

UCNs are phosphors that absorb light in the NIR region and emit in the visible region. The UCNs are usually synthesized with host lattices such as LaF_3, YF_3, Y_2O_3, $LaPO_4$, $NaYF_4$ codoped with trivalent rare earth ions such as Yb^{3+}, Er^{3+} and Tm^{3+} (Wang *et al.* 2006; Guo & Qiao 2009; Lisiecki *et al.* 2009). The host lattice with crystals of yttrium fluoride, such as $NaYF_4$ particles codoped with $Er^{3+}/Yb^{3+}/Tm^{3+}$, was found to be the most efficient in the process of upconversion (Suyver *et al.* 2005, 2006; Schafer *et al.* 2007). The rare earth lanthanides doped in crystal centres of UCNs act as absorber ions and emitter ions. The absorber ion (e.g. Yb^{3+}) is excited by an infrared light source and then transfers this energy non-radiatively to the emitter ion (e.g. Er^{3+} or Tm^{3+}) that radiates a photon. This class of NPs has gained popularity in recent years and has been used for various biological applications such as imaging (Chatterjee *et al.* 2008; Jiang & Zhang 2008), photodynamic therapy (Chatterjee & Yong 2008; Ungun *et al.* 2009), FRET studies (Wang *et al.* 2005*b*; Kuningas *et al.* 2006), biomolecules delivery (Jiang *et al.* 2009), immunoassays (Kuningas *et al.* 2007; Ukonaho *et al.* 2007), immunocytochemistry (Zijlmans *et al.* 1999), immunochromatography (Hampl *et al.* 2001), microarray applications (van de Rijke *et al.* 2001) and DNA detection (Corstjens *et al.* 2001; Wang & Li 2006).

UCNs are usually synthesized at very high temperatures or in organic solvents in the presence of surfactants. These processes produce NPs that are insoluble in water, non-biocompatible and lack functional

Table 1. Comparison of organic dye-doped NPs, QDs and UCNs.

parameter	organic dye-doped NPs	QDs	UCNs
size	50–500 nm	2–10 nm	50–200 nm
autofluorescence	high	high	low
light penetration depth	medium/high	medium/high	high
photodamage	medium/low	medium/low	low
cytotoxicity	medium	high/medium	low
biocompatibility	good	good	good
photostability	low	high	high
excitation wavelength	UV/vis/NIR	UV/NIR	NIR
cost	low/medium	high	low
excitation radiation toxicity	medium/low	medium/low	low
multiplexing assays	n.a.	good	good

groups for conjugation to biomolecules. Wang *et al.* (2006) developed a more efficient hydrothermal synthesis process, where the NPs were synthesized with a PEI coating that makes the particles biocompatible. Other strategies using surfactants such as poly(vinyl pyrrolidone) and oleic acid and encapsulating with polystyrene were also used to obtain enhanced stability, solubility and functionality (Li & Zhang 2006; Li *et al.* 2008; Qian *et al.* 2008*a*).

Fluorescent UCNs have excellent photostability, chemical stability, low toxicity and are biocompatible (Chatterjee *et al.* 2008). The main advantages of these NPs over visible QDs and organic dye doped NPs is their ability to be excited in the NIR region, where autofluorescence is minimal, tissue penetration is maximum and there is minimum photodamage. They also do not exhibit photoblinking, which is a phenomenon observed in QDs. NIR QDs have many comparable properties to UCNs like high penetration depth but they are comparatively costlier than UCNs and more toxic. The upconversion fluorescence output of UCNs is also higher than that of QDs by seven orders of magnitude (Heer *et al.* 2004). Biodistribution of UCNs has been studied and they are cleared from the body mostly by 7 days (Jalil & Zhang 2008). Thus, fluorescent UCNs are becoming a class unto themselves with a lot of advantages over their predecessors and are excellent for biological applications. A comparison of organic dye-doped NPs, QDs and UCNs is presented in table 1.

3. *IN VITRO* IMAGING OF CANCER

To realize the benefits of early cancer diagnosis, highly sensitive and specific assays for biomarkers are needed: a biomarker is an indicator of a particular state, either normal or diseased state of an organism. By critically defining the implication among these biomarkers, it is possible to diagnose and prognosticate cancer based on a patient's molecular profile, leading to personalized and predictive medicine. Within the last several years, lots of articles have described the ability of fluorescent NP probes to accurately and quickly quantify biomarkers on cancer cells or tissue specimens, allowing a non-invasive detection for cancer.

Some receptors or antigens on cell plasma membrane have been studied as cancer biomarkers. Selection of the appropriate receptors or antigen on cancer cells is important for specific cancer diagnosis or receptor-mediated delivery of therapeutic agents. The ideal targeted antigens should have abundant and unique expression on cancer cells, but undetectable or low expression on normal cells. The targeted NPs can be internalized after binding to the antigens, increasing the intracellular concentration of drugs (Goren *et al.* 1996). Plasma membrane antigens on living cells such as integrins (Lieleg *et al.* 2007; Garg *et al.* 2009), folate receptors (Zhang & Huang 2006; Kim *et al.* 2008*a*; Jiang *et al.* 2009), transferrin receptors (Qian *et al.* 2007, 2008*b*) and erbB2/HER2 (Wu *et al.* 2003; Lidke *et al.* 2004; Wartlick *et al.* 2004; Cirstoiu-Hapca *et al.* 2006; Tan *et al.* 2007; Anhorn *et al.* 2008) have been specifically recognized and tracked with fluorescent NP bioconjugates. On the other hand, the choice of targeting moieties that are modified on the NPs is also important to successfully bind the cancer cell and trigger receptor-mediated endocytosis. A variety of affinity agents, such as monoclonal antibodies (mAb; Santra *et al.* 2001; Cirstoiu-Hapca *et al.* 2006; Tan *et al.* 2007), receptor ligands (Zhang & Huang 2006; Huang *et al.* 2007), recognition peptides (Lagerholm *et al.* 2004; Ruan *et al.* 2007) or aptamers (Bagalkot *et al.* 2007), have been used to facilitate the uptake of carriers into target cells. A review outlined the major cancer targets for NP systems (Byrne *et al.* 2008).

For example, HER2, human epidermal growth factor receptor-2, is a potential target as a diagnostic biomarker. The overexpression of HER2 protein has been observed on the plasma membrane of tumours, in particular breast and ovarian cancers, which is related with poor prognosis (Slamon *et al.* 1989; Ross & Fletcher 1999). Fluorescent NPs are conjugated with the intact or derived forms of mAb directed against the extracellular domain of HER2 and used to label cancer cells, offering a potential strategy for HER2-targeted diagnostic imaging. It is reported that poly(DL-lactic acid) NPs (PLA NPs) conjugated with anti-HER2 mAb (trastuzumab, Herceptin) can specifically target SKOV-3 human ovarian cancer cells (overexpressing HER2; Cirstoiu-Hapca *et al.* 2006). A green fluorescent dye, dioctadecyloxacarbo-cyanine perchlorate (Dio), was incorporated into PLA NPs as a fluorescent probe. The internalization of anti-HER2 NPs into SKOV-3 cells was observed in the fluorescent image, representing the efficacy of NPs in active targeting for cancer therapy. Similarly, using the HER2 receptor-specific antibody trastuzumab conjugated to the surface of human serum albumin (HSA) NPs, a specific targeting to HER2-overexpressing cells was reported (Wartlick *et al.* 2004). Recently, HSA NPs conjugated with trastuzumab and loaded with doxorubicin (DOX) drug were developed (Anhorn *et al.* 2008). SK-BR-3 breast cancer cells overexpressing HER2 showed a good cellular binding and uptake of the NPs, as well as a specific and efficient growth inhibition after the intake of NPs.

In addition, QDs are being intensely studied as a class of NP probes for cellular imaging. Wu *et al.* (2003) have used QDs linked to immunoglobulin G (IgG) and streptavidin to label the breast cancer marker HER2 on the surface of fixed and live cancer cells, to stain actin and microtubule fibres in the cytoplasm, and to detect nuclear antigens inside the nucleus (Wu *et al.* 2003). All labelling signals are sensitive and specific for the intended targets at the subcellular level. Using QDs with different emission spectra, QD535 (QDs with emission maximum at 535 nm) and QD630, conjugated to IgG and streptavidin, respectively, HER2 receptor and nuclear antigens in SK-BR-3 cells were simultaneously detected with one excitation wavelength. Therefore, QDs conjugated to different targeting moieties are effective in multiplexing assay. Recent advances in molecular, biological and genetic diagnostic techniques have revealed that cancer is controlled by complex multi-functional mechanisms rather than a single factor. The development of fluorescent NPs may contribute significantly to simultaneous and accurate quantification of several cancer-associated biomarkers on a single cell or a small tumour specimen (Jaiswal *et al.* 2003; Xing *et al.* 2007; Yezhelyev *et al.* 2007; Li *et al.* 2008). For example, Yezhelyev *et al.* (2007) demonstrated the use of multi-colour QDs for quantitative and simultaneous profiling of multiple biomarkers using FFPE (formalin-fixed and paraffin-embedded) breast cancer cells and FFPE clinical tissue specimens. QDs emitting at 525, 565, 605, 655 and 705 nm were directly conjugated to primary Abs against nuclear hormone receptors (ER and PR), cell membrane surface antigens (HER2 and EGFR) and cytoplasmic mTOR protein. The multicolour bioconjugates were used for simultaneous detection of the five clinically significant tumour markers in breast cancer cells, MCF-7 and BT-474 (figure 1). Simultaneous quantification of ER, PR and Her2 receptors correlated closely with the results from traditional methods including immunohistochemistry, western blotting and fluorescence *in situ* hybridization, suggesting that the QD-based technology is well suited for molecular profiling of tumour biomarkers *in vitro*. Similarly, Fountaine *et al.* (2006) successfully stained a variety of differentially expressed antigens in FFPE tonsil tissues with up to five different streptavidin-conjugated QDs simultaneously.

Owing to their novel optical properties, Yb/Er-doped $NaYF_4$ UCNs were used for cellular imaging of cancer. UCNs were conjugated with anti-HER2 antibody and were used to fluorescently label HER2 receptors of SK-BR-3 cells (Jiang *et al.* 2009). The intracellular uptake of UCNs via HER2 receptors was visualized using a confocal fluorescence microscope equipped with an NIR laser. The targeted cellular imaging of UCNs provides a potential for *in vivo* tumour studies by UCNs with excellent optical properties.

4. *IN VIVO* DETECTION OF CANCER

In comparison to the study of living cells in culture, different challenges arise with the increase in complexity and size of a multicellular organism. Conventional *in vivo* imaging methods such as computed tomography (CT) and magnetic resonance (MR) are suitable to delineate morphological features of the tumour, tissue and organs, including the anatomic location, extent and size of the tumour at the macroscopic level (Forstner *et al.* 1995). Despite continuous improvements in spatial resolution with advanced imaging equipment, CT and MR imaging (MRI) have limited sensitivity and ability to provide specific and functional information on the tumour at the microscopic level. A new field of molecular imaging has been developed for better tumour imaging in living systems (Shah *et al.* 2004; Atri 2006; Weissleder 2006). Several molecular imaging techniques such as positron emission tomography (PET), single photon emission CT and optical imaging have shown great promises in non-invasive *in vivo* imaging (Bhushan *et al.* 2008; Perk *et al.* 2008; Shi *et al.* 2008). Especially, fluorescent NPs introduce the possibility of vastly improving sensitivity, resolution and information content of *in vivo* imaging.

To develop NPs for promising tumour imaging and eventually translate it to clinical applications, the following issues should be considered. Firstly, NP imaging probes should emit a strong fluorescence signal to improve the detection sensitivity. NPs with NIR excitation (650–900 nm) are highly preferable for *in vivo* imaging because of their higher penetration depth and minimized tissue autofluorescence compared with UV or visible light (Shah *et al.* 2001; Vogel & Venugopalan 2003). Secondly, NPs should be photostable, allowing real-time and long-time monitoring of cancer progression during cancer therapy. Thirdly, NPs should be modified with stable and high-affinity targeting moieties, achieving specific targeting of tumour tissues and effective loading to cancer cells. Finally, NPs should be appropriately surface modified, to increase the stability and half-life of NPs in circulation.

4.1. Targeting of tumours using nanoparticles

Most anti-cancer agents cannot greatly differentiate between cancerous and normal cells, leading to systemic toxicity and adverse effects. The severe side effects in other tissues greatly limit the maximal allowable dose of the drugs to be systemically delivered in a living system, resulting in inadequate drug concentrations reaching the tumour. NP systems can deliver anti-cancer agents to tumour sites by either passive or active targeting strategy, offering significant benefits to cancer patients (Byrne *et al.* 2008; Wang *et al.* 2008).

Passive targeting takes advantages of the inherent size of NPs and the unique properties of tumour vasculature to enhance the efficacy of drugs. In order to grow beyond 1–2 mm diameter, solid tumours need to increase their surrounding vasculature, in a process known as angiogenesis (Folkman 1990; Folkman & Shing 1992). Angiogenic blood vessels show several abnormalities including a deficiency in pericytes, aberrant basement membrane formation and a relatively high proportion of proliferating cells (Baban & Seymour 1998). The abnormal tumour vasculature results in

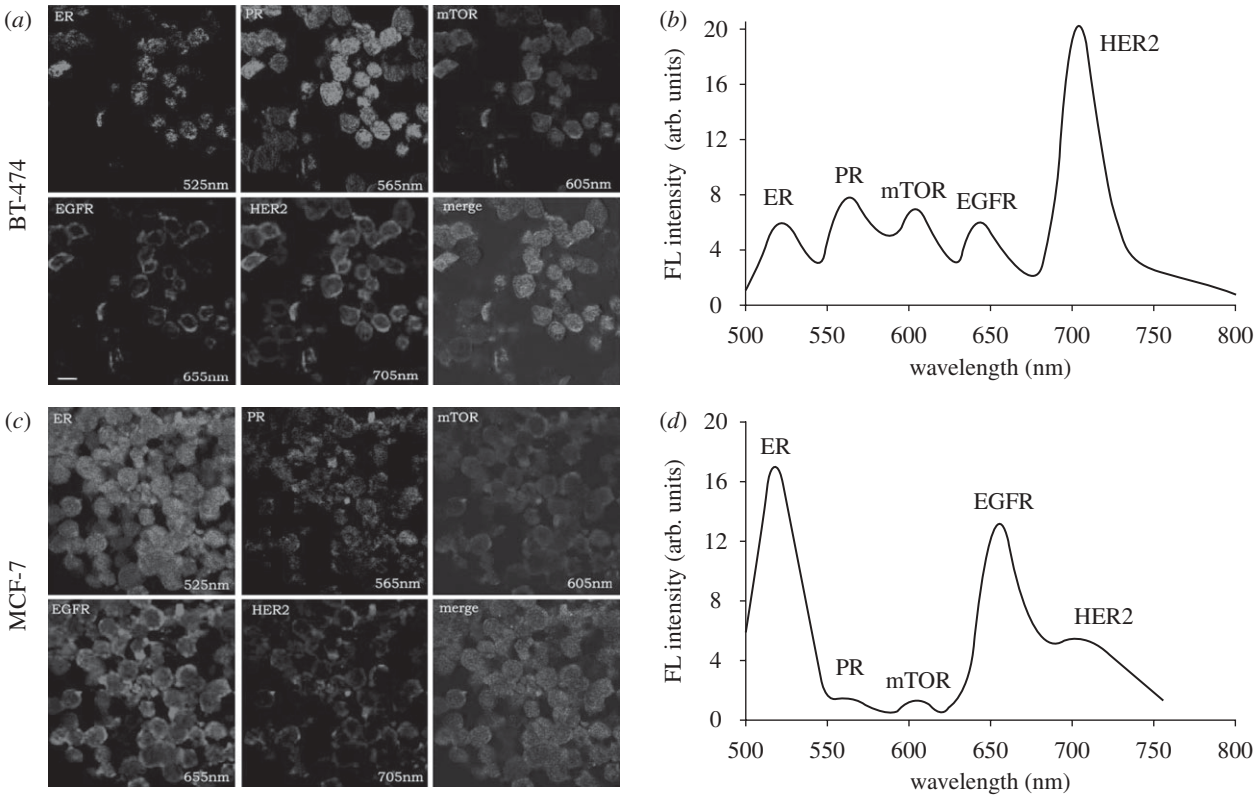

Figure 1. MCF-7 and BT-474 human breast cancer cells stained with QD-Abs against nuclear hormone receptors (ER and PR), cell membrane surface antigens (HER2 and EGFR) and cytoplasmic mTOR protein. (*a*) BT-474 cells showed positive labelling of membrane, cytoplasmic and nuclear antigens indicating expression of all five biomarkers. (*b*) Spectrum of QD emission of a representative BT-474 cell with emission peaks at 525, 565, 605, 655 and 705 nm, confirming the differential expression levels of the tumour biomarkers (not necessarily the same as the average expression levels of a large cell population). (*c*) MCF-7 cells labelled with the same panel of QD-Ab bioconjugates. Spectral deconvolution reveals positive stains of ER, EGFR and HER2. (*d*) Spectrum of QD emission of a representative MCF-7 cell with intensive fluorescent emission at 525 and 655 nm and low signals at 565, 605 and 705 nm (not necessarily the same as the average expression levels of a large cell population). Owing to the nature of spectral deconvolution imaging, (*a*) and (*c*) are pseudo-colour images. Scale bar, 10 μm. Adapted from Yezhelyev *et al.* (2007). Copyright © Wiley-VCH Verlag GmbH & Co. KGaA.

leaky vessels with gap sizes of 200 nm to 1.2 μm between adjacent endothelial cells (Hobbs *et al.* 1998; Allen & Cullis 2004), allowing the extravasation of NPs through these gaps into extravascular spaces. In addition, NPs that gain interstitial access to the tumour have higher retention times than normal tissues because of lack of an effective lymphatic drainage that causes an outward convective interstitial fluid flow in tumours (Baish *et al.* 1996; Baban & Seymour 1998). The leaky vasculature coupled with poor lymphatic drainage induces the enhanced permeability and retention (EPR) effect, resulting in the accumulation of NPs at the tumour site (Jain 2000; Duncan 2003; Brannon-Peppas & Blanchette 2004). There are numbers of studies that display significantly improved therapeutic efficacy of NP drug carriers against different tumour models compared to the free drugs (Nakanishi *et al.* 2000; Satchi-Fainaro *et al.* 2004; Okuda *et al.* 2006; Kim *et al.* 2008*d*). The factors that effect the accumulation of NPs in tumours consist of the size and surface characteristics of NPs, and degree of angiogenesis of the tumour, but it is not well understood yet.

Active targeting is to conjugate targeting moieties to NPs, achieving accumulation of NPs in the tumour sites or individual cancer cells. The targeting moiety, an antibody or ligand, specifically binds to an antigen or receptor overexpressed on the tumour cell surface and assists the NP drug delivery system to selectively and efficiently deliver drugs to tumour sites. The targeted NPs may contribute to the next generation of drug delivery system owing to their increased therapeutic effect (Ulbrich *et al.* 2004; Xu *et al.* 2005; Cheng *et al.* 2007; Diez *et al.* 2009). However, the biodistribution and pharmacokinetics of the uptake of targeted NPs have not yet been well addressed (Pirollo & Chang 2008). Several recent papers have suggested that antibody targeting primarily increases intracellular uptake of NPs and does not increase tumour localization (Kirpotin *et al.* 2006; Bartlett *et al.* 2007; Hussain *et al.* 2007), while other reports indicate that tumour localization is dependent on the antibody targeting (Wu *et al.* 2000; Sundaresan *et al.* 2003). Further studies are clearly needed to understand the systemic delivery of targeted NPs more completely.

4.2. In vivo *tumour imaging*

In vivo diagnostics provide instantaneous data from the patient and allow early detection of cancer and observation of cancer therapy. NPs offer a possibility to produce new medical imaging techniques with higher sensitivity and precision of recognition. Recently, various fluorescent NPs have been used for several types of *in vivo*

animal imaging, including imaging of tumour tissues (Chen *et al.* 2007; Tanisaka *et al.* 2008; Miki *et al.* 2009), angiogenic vasculature (Cai *et al.* 2006; Smith *et al.* 2008) and sentinel lymph nodes (SLNs; Kim *et al.* 2004; Soltesz *et al.* 2004; Zimmer *et al.* 2006). Of the various fluorescent NPs investigated to date, NIR fluorescent NPs are of interest for non-invasive *in vivo* imaging. Organic dye-doped NPs (Chen *et al.* 2007; Tanisaka *et al.* 2008; Miki *et al.* 2009) and QDs (Kim *et al.* 2004; Soltesz *et al.* 2004; Cai *et al.* 2006; Zimmer *et al.* 2006; Smith *et al.* 2008) emitting NIR fluorescence (NIRF) have been widely studied in the last decade. Furthermore, UCNs demonstrated their potential in optical imaging of living animals (Chatterjee *et al.* 2008; Jalil & Zhang 2008).

Tanisaka *et al.* (2008) reported that genuine peptide vesicles, peptosomes, composed of hydrophilic poly(sarcosine) and hydrophobic poly(γ-methyl L-glutamate) were labelled with an NIRF probe, indocyanine green (ICG). NIRF imaging of a small cancer on mouse by using peptosome as a nanocarrier was successful due to the EPR effect of the peptosome. Similarly, Miki *et al.* (2009) demonstrated that ICG labelled amphiphilic block copolymers could be efficiently accumulated in tumours over two weeks via optical imaging of live animals. However, NIR QD spectroscopic properties can be exploited here to achieve deeper penetration than the available NIR dyes (Xing & Rao 2008). Kim *et al.* (2004) synthesized NIR type II QDs and applied them to SLN mapping in cancer surgery of animals. Injection of only 400 pmol of NIR QD permits SLNs 1 cm deep to be imaged easily in real time using excitation fluorescence rates of only 5 mW cm^{-2}. The utilization of NIR QDs provides the surgeon with direct visual guidance throughout the entire SLN mapping procedure, minimizes incision and dissection inaccuracies and permits real-time confirmation of complete resection. Two years later, the same group reported the synthesis of a size series of NIR QDs smaller than 10 nm at hydrodynamic diameters and their utility *in vivo* by imaging multiple, sequential lymph nodes and showing extravasation from the vasculature in rat models (Zimmer *et al.* 2006). Furthermore, Cai *et al.* (2006) reported the *in vivo* targeting and imaging of tumour vasculature using arginine–glycine–aspartic acid (RGD) peptide-labelled NIR QDs. QD705 (emission maximum at 705 nm) modified with RGD peptide that specifically targets integrin $\alpha_v\beta_3$-positive tumour vasculature was intravenously administered into mice bearing subcutaneous U87MG human glioblastoma tumours. The tumour fluorescence intensity reached maximum at 6 h post-injection with good contrast, opening up new perspectives for integrin-targeted NIR optical imaging and imaging-guided surgery. More recently, the same group exploited intravital microscopy with subcellular (approx. 0.5 μm) resolution to examine the binding of neovascularly targeted NIR QDs to tumour vasculature via direct cellular-level visualization in living mice (Smith *et al.* 2008).

In addition, while upconversion technology has been known for several decades, the use of UCNs in biology is a relatively recent phenomenon. Zhang's group report that PEI coated $NaYF_4$:Yb,Er UCNs are stable in physiological-buffered saline, non-toxic to bone marrow stem cells and resistant to photo-bleaching (Chatterjee *et al.* 2008). The UCNs and QDs are injected intradermally and intramuscularly into some tissues either near the body surface or deep in the body of rats. UCNs showed visible fluorescence exposed to an NIR laser, but QDs do not emit fluorescence exposed to UV light (figure 2). Similarly, silica-coated $NaYF_4$:Yb,Er UCNs with strong NIR-to-visible fluorescence were injected intravenously to investigate their biocompatibility and tissue distribution (Jalil & Zhang 2008). The results revealed that UCNs displayed good *in vitro* and *in vivo* biocompatibility, demonstrating their potential applications in both cellular and animal imaging systems.

4.3. Dual-modality imaging

The application of optical imaging for *in vivo* imaging is hampered by limited tissue penetration depth and lack of anatomic resolution and spatial information. Although NIRF imaging can be used to improve penetration depth and detection sensitivity, other imaging modalities, such as MRI and PET, are much better for high spatial resolution, tomographic capability and unlimited tissue penetration depth (Massoud & Gambhir 2003). Thus, a combination of imaging modalities that could allow one to extract anatomical, physiological and molecular information would be advantageous for *in vivo* imaging (Moore *et al.* 2004; Medarova *et al.* 2006; Cai *et al.* 2007; Lee *et al.* 2007; Simberg *et al.* 2007; Yang *et al.* 2007; Chen *et al.* 2008; Medarova *et al.* 2009).

For example, Moore *et al.* (2004) synthesized and tested specific and selective accumulation of a novel dual-modal imaging probe in underglycosylated mucin-1 (uMCU-1) antigen-positive subcutaneous tumour *in vivo*. The dual-modal probe consists of cross-linked iron oxide (CLIO) NP as an MRI contrast agent, modified with Cy5.5 dye as NIRF optical probe, and carrying uMUC-1 targeting peptides attached to the dextran coat of NP. Accumulation of the probe in the tumours after intravenous injection was detected by the decrease in signal intensity on T2-weighted MR images and by the bright NIRF signal on optical images. In 2006, the same group demonstrated that the dual-modal imaging probe could not only detect orthotopically implanted preclinical models of adenocarcinomas but could also track tumour response to 5-fluorouracil, a clinically used chemotherapeutic agent, *in vivo* in real time (Medarova *et al.* 2006). More recently, they further proved that tumour delta-T2 was significantly reduced after treatment with DOX drug, indicating a lower accumulation of probe and reflecting the reduced expression of uMUC-1 in orthotopic human breast tumour (Medarova *et al.* 2009). This dual-modality approach delivers information not only about change in tumour size but also about target antigen expression *in vivo*. In addition, Cai *et al.* (2007) and Chen *et al.* (2008) developed a QD-based dual-function PET/NIRF probe that allows the accurate assessment of the tumour-targeting efficacy of QDs. Yang *et al.* (2007) report the synthesis of core-cross-linked polymeric micelles (CCPMs) entrapped with Cy7 and labelled

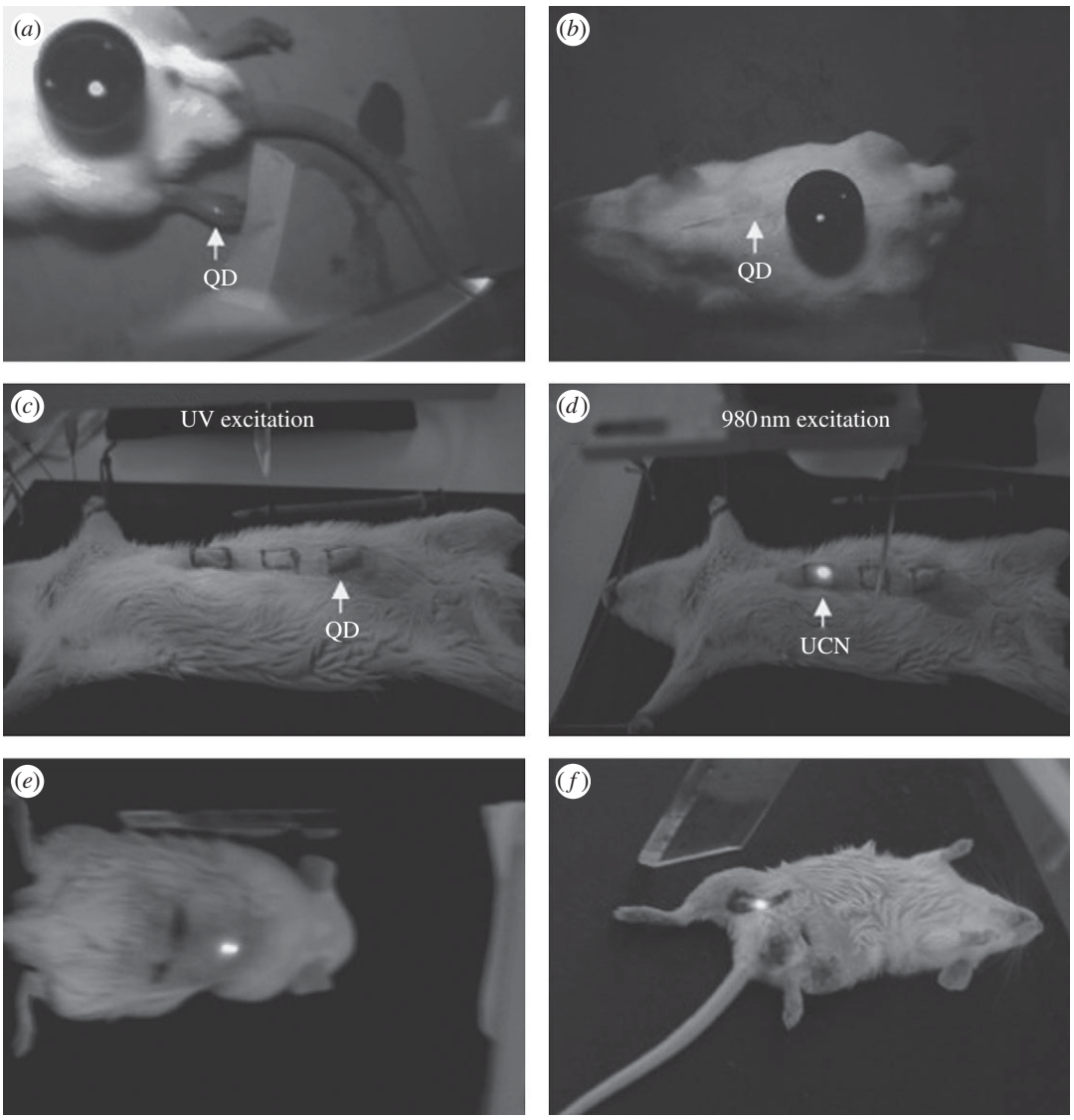

Figure 2. *In vivo* imaging of rat: QDs injected into translucent skin of (*a*) foot show fluorescence, but not through thicker skin of (*b*) back or (*c*) abdomen; PEI/$NaYF_4$:Yb,Er NPs injected below (*d*) abdominal skin, (*e*) thigh muscles or (*f*) skin of back show luminescence. QDs on a black disc in (*a*,*b*) are used as the control. Adapted from Chatterjee *et al.* (2008). Copyright © 2008 Elsevier.

with ^{111}In, and significant accumulation of CCPMs in human breast tumour xenografts via both NIRF optical and gamma imaging techniques.

5. MULTI-FUNCTIONAL NANOPARTICLES

NPs have a large surface area to accommodate a large number or a wide range of surface functional groups allowing chemical conjugation to multiple diagnostic and therapeutic agents as well as targeting moieties. This may enable the development of multi-functional 'smart' NPs for simultaneous tumour imaging and treatment, a major goal in cancer research. For example, a core particle could be conjugated to a specific targeting component that provides preferential accumulation of NPs in the target tumour. Simultaneously, the same particles could be linked to a therapeutic agent to inhibit the tumour growth and an imaging agent to monitor the drug transport process (figure 3). Although these new materials are of great interest, most of the studies are still at an early or proof-of-concept stage with cultured cancer cells and *in vivo* imaging and are not relevant to the treatment of solid tumours.

Fluorescent NPs have shown a great promise for cellular labelling and *in vivo* imaging of cancer. Monitoring of the biodistribution of particles can be done in real time. Drug-loaded NPs also have been used for treating cancer in animal models and even in clinical trials. Owing to their size and structural similarities, it is possible that they can be integrated and multi-functional NPs can be constructed to simultaneously track therapeutic delivery and treat cancer.

Multi-functional NPs are prepared with organic materials and/or inorganic materials. Organic liposomes, polymer NPs and carbon nanotubes have been used as drug carriers that are loaded with therapeutic agents (anti-cancer drugs, protein, nucleic acid, photothermal agents, etc.) and modified with target moieties and imaging agents (magnetic NPs, organic dyes, QDs,

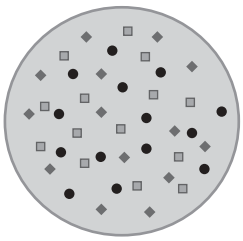

Figure 3. Multi-functional NP. The multifunctional NP has the capability to simultaneously carry therapeutic agents (squares), imaging contrast agents (diamonds) and targeting moieties (circles). The NP can be used for specific delivery of anti-cancer agents, tracking of therapeutic delivery and detection of treatment effects in real time.

gold NPs, etc.; Huang *et al.* 2007; Guo *et al.* 2008; Kim *et al.* 2008*c*; Weng *et al.* 2008). On the other hand, inorganic NPs, such as QDs, magnetic NPs and lanthanide-doped UCNs, can be used as a central core that defines their fluorescent, magnetic and optical properties, and then modified with polymer or silica coating in order to improve their biostability and biocompatibility, and finally loaded with therapeutic agents and conjugated with targeting moieties (Bagalkot *et al.* 2007; Kim *et al.* 2008*b*; Yezhelyev *et al.* 2008).

NPs are known for their versatility, and various multi-functional NPs capable of simultaneous imaging, delivery, etc. are used. For example, a multi-functional micelle was developed for *in vitro* cancer cell targeting, distribution imaging and anti-cancer drug delivery (Huang *et al.* 2007). The mixed micelles were prepared by dialysis from graft copolymer and diblock copolymer, and then DOX, an anti-cancer drug, was incorporated into the inner core of micelles. FITC-labelled micelles exhibited a specific tumour targeting mediated by asialoglycoprotein receptors and a clear distribution in the cytoplasm. DOX drugs released from micelles have strong effects on the viability of tumour cells HepG2. Another polymeric NP, PLGA, was used as a matrix for loading magnetite nanocrystals or QDs, in addition to DOX drugs (Kim *et al.* 2008*c*). Pegylated folate was coated on the surface of NPs for active targeting of cancer cells. Cancer cell-targeted MRI and optical imaging, as well as drug delivery, were successfully demonstrated by the multi-functional polymer NPs. Furthermore, several kinds of targeted delivery system were developed for tumour labelling applications *in vivo*. Liposomes, the most clinically established NPs for drug delivery, were conjugated to luminescent QDs and tumour-targeting moieties (e.g. anti-Her2 single chain Fv fragments) and were loaded with DOX (Weng *et al.* 2008). DOX-loaded NPs showed efficient anti-cancer activity in HER2-overexpressing SK-BR-3 cells. The QD-conjugated immunoliposome-based NPs were able to provide tumour cell imaging and *in vivo* localization at tumour sites after their intravenous injection. Owing to the superior optical properties (e.g. brightness and photostability) of QDs, they were also functionalized to the outer surface of carbon nanotubes for *in vivo* trackable delivery. Shi *et al.* (2007*a*) synthesized CdSe/ZnS QD-conjugated carbon nanotubes (CNT-QD) by a unique plasma coating method and demonstrated their potential applications in cancer diagnosis. One year later, the same group reported that CNT-QD exhibited strong luminescence suitable for non-invasive optical *in vivo* imaging with an NIR emission around 800 nm (Guo *et al.* 2008). Paclitaxel, an anti-tumour agent, loaded CNT-QD demonstrated *in vitro* anti-tumour efficacy against human PC-3MM2 prostate cancer cells. However, the nanotubes will not be used for *in vivo* tumour treatment unless they can lead paclitaxel to tumour specifically after intravenous injection.

Among these various inorganic nanomaterials, silica or mesoporous silica materials have been intensively investigated for their potential application as delivery vehicles (Lai *et al.* 2003; Lu *et al.* 2007; Slowing *et al.* 2007) and imaging probes (Huang *et al.* 2005; Yi *et al.* 2005; Lin *et al.* 2006; Selvan *et al.* 2007; Wu *et al.* 2008; Lee *et al.* 2009) owing to their considerable biocompatibility and easy surface functionalization. However, these materials have not been used for *in vivo* simultaneous imaging and drug delivery. Kim *et al.* (2008*b*) presented discrete, monodisperse and precisely size-controllable core–shell mesoporous silica NPs smaller than 100 nm. A single Fe_3O_4 nanocrystal core was used as an MRI agent, and FITC or RITC incorporated covalently into the silica wall was used as a fluorescent imaging agent. NPs were verified to accumulate preferentially at tumour sites through the EPR effect after intravenous injection. To examine the drug delivery of the NPs, the cytotoxic effect of DOX-loaded NPs was tested on SK-BR-3 cells, indicating that mesoporous silica NPs have a potential for drug delivery into cancer cells to induce cell death. In another example, Bagalkot *et al.* (2007) reported a novel QD-aptamer-DOX conjugate (QD-Apt(DOX)) as a targeted cancer imaging, therapy and sensing system. By functionalizing the surface of fluorescent QD with the A10 RNA aptamer, which recognizes the prostate-specific membrane antigen, and intercalating DOX into the double-stranded CG sequence of the aptamer, a targeted QD-Apt(DOX) conjugate with reversible self-quenching properties based on a Bi-FRET mechanism was developed. Two donor–quencher pairs of FRET occurred in this construct, as the QD fluorescence was quenched by DOX, and DOX was quenched by aptamers. The multi-functional NP system can deliver DOX to the targeted prostate cancer cells and sense the release of DOX by activating the fluorescence of the QD, which concurrently images the cancer cells and inhibits the growth of specific prostate cancer cell lines. However, the current design is not sufficient for *in vivo* use unless the drug-loading capacity can be greatly increased.

Multi-functional NPs can also be used for small interference RNA (siRNA) delivery and imaging. RNA interference (RNAi) has emerged as a powerful technology for sequence-specific silencing of genes and holds great potential as a new treatment paradigm for human diseases amenable to manipulation at the gene expression level (Fire *et al.* 1998; Elbashir *et al.* 2001; Bumcrot *et al.* 2006; Rana 2007; Castanotto & Rossi 2009; Kurreck 2009). The basic mechanism of RNAi is thought to be a multi-step process where siRNA (usually double-strand RNA 21–23 nucleotides in length) with

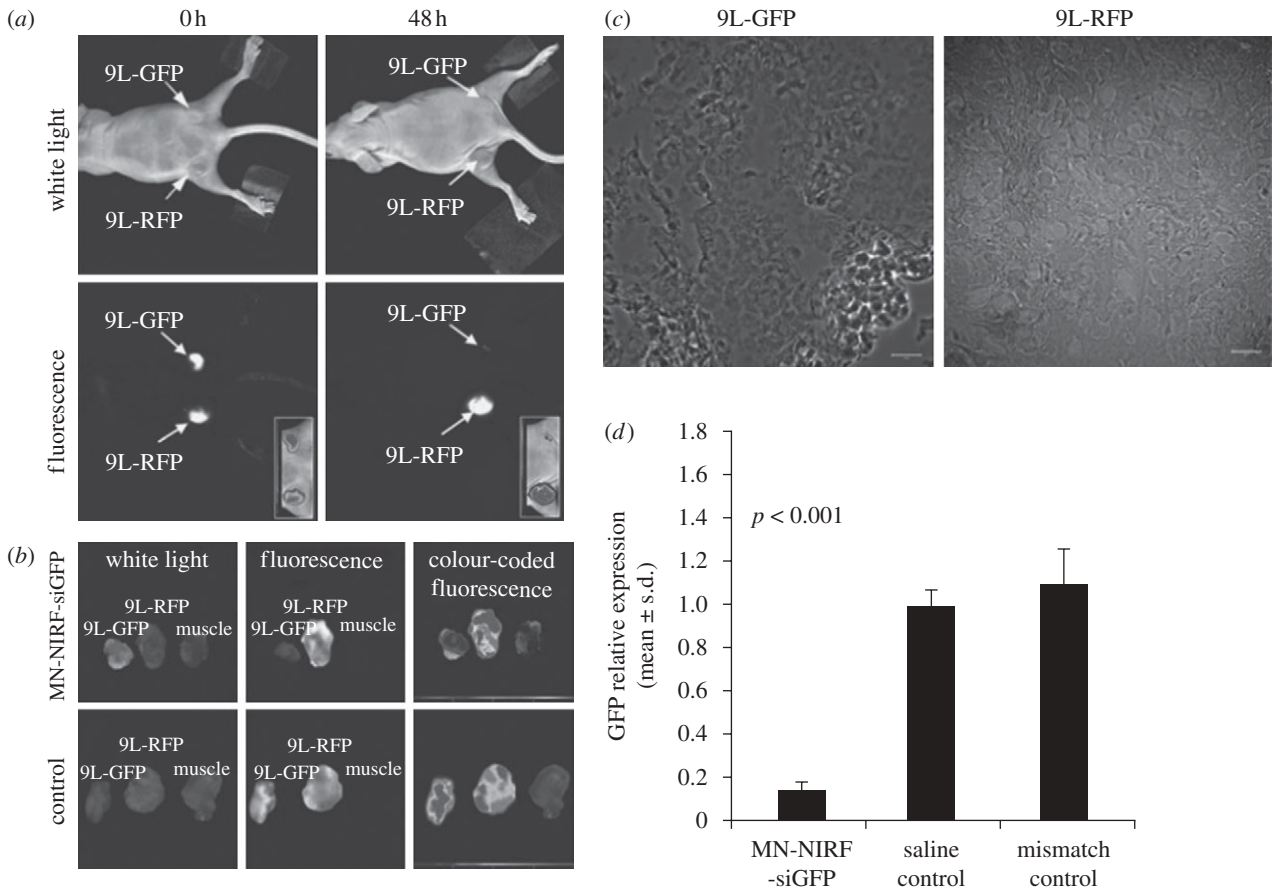

Figure 4. *In vivo* imaging of MN-NIRF-siGFP silencing in tumours. (*a*) *In vivo* NIRF optical imaging of mice bearing bilateral 9L-GFP and 9L-RFP (GFP, green fluorescent protein; RFP, red fluorescent protein) tumours 48 h after intravenous probe injection. There was a marked decrease in 9L-GFP-associated fluorescence ($P\frac{1}{4}$ 0.0083) and no change in 9L-RFP fluorescence. To generate GFP/RFP reconstructions, GFP and RFP images were acquired separately and then merged. (*b*) Correlative *ex vivo* fluorescence optical imaging showed a significant drop in fluorescence intensity in 9L-GFP tumours ($P\frac{1}{4}$ 0.0036). There was no evidence of silencing in saline-injected controls. (*c*) Confocal microscopy of frozen tumour sections indicated the presence of the probe in both 9L-GFP and 9L-RFP tumours. However, in GFP tumours, GFP fluorescence was predominantly at background levels. Note that the 9L-RFP section produced bright fluorescence. Scale bar, 20 mm. (*d*) Quantitative RT–PCR analysis of GFP expression performed on total RNA extracted from 9L-GFP tumours from mice injected with either MN-NIRF-siGFP, a mismatch control or saline solution. Representative data are shown. Adapted from Medarova *et al.* (2007). Copyright © 2007 Macmillan Publishers Ltd.

sequences complementary to a gene's sequence suppresses the activity of the gene by bringing about the degradation of the corresponding messenger RNA (mRNA), thus blocking the translation of the mRNA into proteins (Fire *et al.* 1998; Elbashir *et al.* 2001; Hannon 2002; Martinez *et al.* 2002). The major obstacle to therapeutic application of RNAi, however, is the delivery of siRNA to the target tissue owing to its fast degradation in the physiological environment, poor cellular uptake, inefficient endosomal escape, insufficient dissociation from the carrier and lack of targeting ability. Numerous siRNA delivery carriers have been developed such as liposomes (Hassani *et al.* 2005; Landen *et al.* 2005; Sonoke *et al.* 2008; Villares *et al.* 2008), polymers (Takeshita *et al.* 2005; Urban-Klein *et al.* 2005; Xiong *et al.* 2009), inorganic NPs (Liu *et al.* 2007*b*; Medarova *et al.* 2007), aptamer–siRNA chimaeras (McNamara *et al.* 2006), cholesterol-conjugated siRNAs (Soutschek *et al.* 2004) and protamine–antibody fusion protein (Song *et al.* 2005). Additionally, there is a need for a method to non-invasively track and monitor siRNA delivery to tissues of interest in order to achieve minimally invasive administration in clinical application. Some typical strategies have been applied to optical tracking of siRNA, involving fluorescently end-modified siRNAs (Howard *et al.* 2006), bioluminescence imaging of siRNA-mediated silencing (McCaffrey *et al.* 2002; Muratovska & Eccles 2004; Takeshita *et al.* 2005) and co-transfecting siRNA with fluorescent NPs (Medarova *et al.* 2007; Tan *et al.* 2007; Yezhelyev *et al.* 2008). Therefore, a multi-functional system is developed to simultaneously deliver and image siRNA for *in vitro* and *in vivo* detection.

For example, Tan *et al.* (2007) used chitosan NPs with encapsulated QDs and surface-conjugated anti-HER2 antibody for targeted delivery of HER2/neu siRNA into HER2-overexpressing SK-BR-3 breast cancer cells. Using such a construct, the intracellular delivery of siRNA was monitored by the presence of fluorescent QDs in the chitosan NPs and gene silencing effects of conjugated siRNA were also established using the luciferase and HER2 ELISA assay. Similarly,

Yezhelyev *et al.* (2008) reported that QDs were used as a nanometre-sized scaffold to conjugate siRNA for real-time tracking and 10- to 20-fold improvement in gene-silencing efficiency. The main finding is that a proton-sponge layer formed on the QD surface by balancing two function groups (carboxylic acid and tertiary amine) leads to efficient siRNA release from acidic endosomes and into cytoplasm. As a result, gene silencing activity is improved by 10- to 20-fold and cell toxicity is reduced by 5- to 6-fold in MDA-MB-231 cells (in comparison with the current siRNA delivery agents). As another example, silica-coated $NaYF_4$:Yb,Er UCNs can serve as a multi-functional system for simultaneous imaging and delivery of siRNA *in vitro* (Jiang *et al.* 2009). siRNA was attached to anti-Her2 antibody-conjugated UCNs and the delivery of these NPs to SK-BR-3 cells overexpressing HER2 receptors was visualized using confocal microscopy. Meanwhile, a luciferase assay was established to confirm the gene-silencing effect of delivered siRNA. However, they have only shown applicability in cell culture, but not yet in living animals. For *in vivo* cancer therapy, Medarova *et al.* (2007) described the synthesis and characterization of multi-functional NPs for *in vivo* transfer of siRNA and the simultaneous imaging of its accumulation in tumours by high-resolution MRI and NIR *in vivo* optical imaging (NIRF). The NPs used CLIO NPs as a core and MRI contrast agent, Cy5.5 dye labelled on the surface as an NIRF optical agent and siRNA duplex conjugated to target a gene of interest. Myristoylated polyarginine peptides were also conjugated on the surface serving as a membrane translocation module. In a series of experiments targeting model (green fluorescence protein) and therapeutic genes (survivin), they found that the delivery system could be monitored *in vivo* by MRI and optical imaging. In addition, the silencing process of delivered siRNA was able to be corroborated by proof-of-principle optical imaging and further confirmed by histological data (figure 4). Overall, the new approach could advance the development and optimization of cancer therapeutic product, siRNA. However, the 'smart' multi-functional NPs are still in development and have only recently shown applicability in imaging in living animals, but not yet in *in vivo* tumour therapy.

6. CONCLUSION

Although nanotechnology is still at an early stage of development, the possibilities for new therapies using this technology to treat cancer seem to be very numerous. Fluorescent NPs appear very promising as novel tools for highly sensitive optical imaging of cancer at cellular and animal levels. Furthermore, the emerging development in novel multi-functional NPs, which combine different functions in one particle, provides new potential for clinical therapies and diagnostics and undoubtedly will make an impact on cancer therapy. With this promising progress in the development of fluorescent NP-guided cancer therapy, it is imperative to constantly improve the fundamental understanding of designing and applying NPs for diagnosis, treatment or the combination of imaging and therapeutics in different clinical situations. However, our limited knowledge on the toxicity of these NPs limits us from exploiting their full potential in clinical applications. Their potential toxicity and their possible incompatibility may result in disorders such as inflammation, immunoreaction or even cancer. The mechanisms of those effects are not well studied yet, but should depend more on whether their accumulation in specific organs occurs because such a deposition of NPs could provoke intracellular changes that might affect cell integrity and hence organ function. Thus, more studies are needed to explore these aspects and new methods that improve the biocompatibility of NPs should be developed to reduce the undesirable side effects. Once these questions have been addressed, optimized NPs with improved selectivity, efficiency and safety could be designed and applied for the diagnosis and treatment of cancer.

The authors acknowledge financial support from A*STAR BMRC (R-397-000-062-305) and the National University of Singapore.

REFERENCES

Allen, T. M. & Cullis, P. R. 2004 Drug delivery systems: entering the mainstream. *Science* **303**, 1818–1822. (doi:10.1126/science.1095833)

Anhorn, M. G., Wagner, S., Kreuter, J., Langer, K. & von Briesen, H. 2008 Specific targeting of HER2 overexpressing breast cancer cells with doxorubicin-loaded trastuzumab-modified human serum albumin nanoparticles. *Bioconjug. Chem.* **19**, 2321–2331. (doi:10.1021/bc8002452)

Atri, M. 2006 New technologies and directed agents for applications of cancer imaging. *J. Clin. Oncol.* **24**, 3299–3308. (doi:10.1200/JCO.2006.06.6159)

Baban, D. F. & Seymour, L. W. 1998 Control of tumour vascular permeability. *Adv. Drug Deliv. Rev.* **34**, 109–119. (doi:10.1016/S0169-409X(98)00003-9)

Bagalkot, V., Zhang, L., Levy-Nissenbaum, E., Jon, S., Kantoff, P. W., Langer, R. & Farokhzad, O. C. 2007 Quantum dot–aptamer conjugates for synchronous cancer imaging, therapy, and sensing of drug delivery based on bi-fluorescence resonance energy transfer. *Nano Lett.* **7**, 3065–3070. (doi:10.1021/nl071546n)

Baish, J. W., Gazit, Y., Berk, D. A., Nozue, M., Baxter, L. T. & Jain, R. K. 1996 Role of tumor vascular architecture in nutrient and drug delivery: an invasion percolation-based network model. *Microvasc. Res.* **51**, 327–346. (doi:10.1006/mvre.1996.0031)

Bang, J. H., Suh, W. H. & Suslick, K. S. 2008 Quantum dots from chemical aerosol flow synthesis: preparation, characterization, and cellular imaging. *Chem. Mater.* **20**, 4033–4038. (doi:10.1021/cm800453t)

Bartlett, D. W., Su, H., Hildebrandt, I. J., Weber, W. A. & Davis, M. E. 2007 Impact of tumor-specific targeting on the biodistribution and efficacy of siRNA nanoparticles measured by multimodality *in vivo* imaging. *Proc. Natl Acad. Sci. USA* **104**, 15 549–15 554. (doi:10.1073/pnas.0707461104)

Bhushan, K. R., Misra, P., Liu, F., Mathur, S., Lenkinski, R. E. & Frangioni, J. V. 2008 Detection of breast cancer microcalcifications using a dual-modality SPECT/NIR fluorescent probe. *J. Am. Chem. Soc.* **130**, 17 648–17 649. (doi:10.1021/ja807099S)

Brannon-Peppas, L. & Blanchette, J. O. 2004 Nanoparticle and targeted systems for cancer therapy. *Adv. Drug Deliv. Rev.* **56**, 1649–1659. (doi:10.1016/j.addr.2004.02.014)

Bumcrot, D., Manoharan, M., Koteliansky, V. & Sah, D. W. Y. 2006 RNAi therapeutics: a potential new class of pharmaceutical drugs. *Nat. Chem. Biol.* **2**, 711–719. (doi:10.1038/nchembio839)

Byrne, J. D., Betancourt, T. & Brannon-Peppas, L. 2008 Active targeting schemes for nanoparticle systems in cancer therapeutics. *Adv. Drug Del. Rev.* **60**, 1615–1626. (doi:10.1016/j.addr.2008.08.005)

Cai, W. B., Shin, D. W., Chen, K., Gheysens, O., Cao, Q. Z., Wang, S. X., Gambhir, S. S. & Chen, X. Y. 2006 Peptide-labeled near-infrared quantum dots for imaging tumor vasculature in living subjects. *Nano Lett.* **6**, 669–676. (doi:10.1021/nl052405t)

Cai, W. B., Chen, K., Li, Z. B., Gambhir, S. S. & Chen, X. Y. 2007 Dual-function probe for PET and near-infrared fluorescence imaging of tumor vasculature. *J. Nucl. Med.* **48**, 1862–1870. (doi:10.2967/jnumed.107.043216)

Castanotto, D. & Rossi, J. J. 2009 The promises and pitfalls of RNA-interference-based therapeutics. *Nature* **457**, 426–433. (doi:10.1038/nature07758)

Chatterjee, D. K. & Yong, Z. 2008 Upconverting nanoparticles as nanotransducers for photodynamic therapy in cancer cells. *Nanomedicine* **3**, 73–82. (doi:10.2217/17435889.3.1.73)

Chatterjee, D. K., Rufalhah, A. J. & Zhang, Y. 2008 Upconversion fluorescence imaging of cells and small animals using lanthanide doped nanocrystals. *Biomaterials* **29**, 937–943. (doi:10.1016/j.biomaterials.2007.10.051)

Chen, J., Corbin, I. R., Li, H., Cao, W. G., Glickson, J. D. & Zheng, G. 2007 Ligand conjugated low-density lipoprotein nanoparticles for enhanced optical cancer imaging *in vivo*. *J. Am. Chem. Soc.* **129**, 5798–5799. (doi:10.1021/ja069336k)

Chen, K., Li, Z. B., Wang, H., Cai, W. B. & Chen, X. Y. 2008 Dual-modality optical and positron emission tomography imaging of vascular endothelial growth factor receptor on tumor vasculature using quantum dots. *Eur. J. Nucl. Med. Mol. Imaging* **35**, 2235–2244. (doi:10.1007/s00259-008-0860-8)

Cheng, J. *et al.* 2007 Formulation of functionalized PLGA-PEG nanoparticles for *in vivo* targeted drug delivery. *Biomaterials* **28**, 869–876. (doi:10.1016/j.biomaterials.2006.09.047)

Cho, K. J., Wang, X., Nie, S. M., Chen, Z. & Shin, D. M. 2008 Therapeutic nanoparticles for drug delivery in cancer. *Clin. Cancer Res.* **14**, 1310–1316. (doi:10.1158/1078-0432.CCR-07-1441)

Cirstoiu-Hapca, A., Bossy-Nobs, L., Buchegger, F., Gurny, R. & Delie, F. 2006 Differential tumor cell targeting of anti-HER2 (Herceptin (R)) and anti-CD20 (Mabthera (R)) coupled nanoparticles. In *6th European Workshop on Particulate Systems*. Geneva, Switzerland: Elsevier Science.

Corstjens, P., Zuiderwijk, M., Brink, A., Li, S., Feindt, H., Neidbala, R. S. & Tanke, H. 2001. Use of up-converting phosphor reporters in lateral-flow assays to detect specific nucleic acid sequences: a rapid, sensitive DNA test to identify human papillomavirus type 16 infection. In *33rd Annual Oak Ridge Conf.* Seattle, WA: American Association for Clinical Chemistry.

Dabbousi, B. O., RodriguezViejo, J., Mikulec, F. V., Heine, J. R., Mattoussi, H., Ober, R., Jensen, K. F. & Bawendi, M. G. 1997 (CdSe)ZnS core-shell quantum dots: synthesis and characterization of a size series of highly luminescent nanocrystallites. *J. Phys. Chem. B* **101**, 9463–9475. (doi:10.1021/jp971091y)

Diez, S., Navarro, G. & de Ilarduya, C. T. 2009 *In vivo* targeted gene delivery by cationic nanoparticles for treatment of hepatocellular carcinoma. *J. Gene Med.* **11**, 38–45. (doi:10.1002/jgm.1273)

Dubertret, B., Skourides, P., Norris, D. J., Noireaux, V., Brivanlou, A. H. & Libchaber, A. 2002 *In vivo* imaging of quantum dots encapsulated in phospholipid micelles. *Science* **298**, 1759–1762. (doi:10.1126/science.1077194)

Duncan, R. 2003 The dawning era of polymer therapeutics. *Nat. Rev. Drug Discov.* **2**, 347–360. (doi:10.1038/nrd1088)

Elbashir, S. M., Harborth, J., Lendeckel, W., Yalcin, A., Weber, K. & Tuschl, T. 2001 Duplexes of 21-nucleotide RNAs mediate RNA interference in cultured mammalian cells. *Nature* **411**, 494–498. (doi:10.1038/35078107)

Ferrari, M. 2005 Cancer nanotechnology: opportunities and challenges. *Nat. Rev. Cancer* **5**, 161–171. (doi:10.1038/nrc1566)

Fire, A., Xu, S. Q., Montgomery, M. K., Kostas, S. A., Driver, S. E. & Mello, C. C. 1998 Potent and specific genetic interference by double-stranded RNA in *Caenorhabditis elegans*. *Nature* **391**, 806–811. (doi:10.1038/35888)

Folkman, J. 1990 What is the evidence that tumors are angiogenesis dependent? *J. Natl Cancer Inst.* **82**, 4–6. (doi:10.1093/jnci/82.1.4)

Folkman, J. & Shing, Y. 1992 Angiogenesis. *J. Biol. Chem.* **267**, 10 931–10 934.

Forstner, R., Hricak, H. & White, S. 1995 CT and MRI of ovarian-cancer. *Abdom. Imaging* **20**, 2–8. (doi:10.1007/BF00199633)

Fountaine, T. J., Wincovitch, S. M., Geho, D. H., Garfield, S. H. & Pittaluga, S. 2006 Multispectral imaging of clinically relevant cellular targets in tonsil and lymphoid tissue using semiconductor quantum dots. *Mod. Pathol.* **19**, 1181–1191. (doi:10.1038/modpathol.3800628)

Gao, X. H., Cui, Y. Y., Levenson, R. M., Chung, L. W. K. & Nie, S. M. 2004 *In vivo* cancer targeting and imaging with semiconductor quantum dots. *Nat. Biotechnol.* **22**, 969–976. (doi:10.1038/nbt994)

Gao, F., Tang, L. J., Dai, L. & Wang, L. 2007 A fluorescence ratiometric nano-pH sensor based on dual-fluorophore-doped silica nanoparticles. *Spectrochim. Acta Part A Mol. Biomol. Spectrosc.* **67**, 517–521. (doi:10.1016/j.saa.2006.08.009)

Garg, A., Tisdale, A. W., Haidari, E. & Kokkoli, E. 2009 Targeting colon cancer cells using PEGylated liposomes modified with a fibronectin-mimetic peptide. *Int. J. Pharm.* **366**, 201–210. (doi:10.1016/j.ijpharm.2008.09.016)

Gerion, D., Pinaud, F., Williams, S. C., Parak, W. J., Zanchet, D., Weiss, S. & Alivisatos, A. P. 2001 Synthesis and properties of biocompatible water-soluble silica-coated CdSe/ZnS semiconductor quantum dots. *J. Phys. Chem. B* **105**, 8861–8871. (doi:10.1021/jp0105488)

Goldman, E. R., Balighian, E. D., Kuno, M. K., Labrenz, S., Tran, P. T., Anderson, G. P., Mauro, J. M. & Mattoussi, H. 2001. Luminescent quantum dot-adaptor protein-antibody conjugates for use in fluoroimmunoassays. In *10th Int. Conf. on II–VI Compounds*. Bremen, Germany: Wiley-VCH Verlag.

Goren, D., Horowitz, A. T., Zalipsky, S., Woodle, M. C., Yarden, Y. & Gabizon, A. 1996 Targeting of stealth liposomes to erbB-2 (Her/2) receptor: *in vitro* and *in vivo* studies. *Br. J. Cancer* **74**, 1749–1756.

Grodzinski, P., Silver, M. & Molnar, L. K. 2006 Nanotechnology for cancer diagnostics: promises and challenges. *Expert Rev. Mol. Diagn.* **6**, 307–318. (doi:10.1586/14737159.6.3.307)

Guo, Y. *et al.* 2008 *In vivo* imaging and drug storage by quantum-dot-conjugated carbon nanotubes. *Adv. Funct. Mater.* **18**, 2489–2497. (doi:10.1002/adfm.200800406)

Guo, H. & Qiao, Y. M. 2009 Preparation, characterization, and strong upconversion of monodisperse Y_2O_3:Er^{3+},Yb^{3+} microspheres. *Opt. Mater.* **31**, 583–589. (doi:10.1016/j.optmat.2008.06.011)

Hampl, J., Hall, M., Mufti, N. A., Yao, Y. M. M., MacQueen, D. B., Wright, W. H. & Cooper, D. E. 2001 Upconverting phosphor reporters in immunochromatographic assays. *Anal. Biochem.* **288**, 176–187. (doi:10.1006/abio.2000.4902)

Hannon, G. J. 2002 RNA interference. *Nature* **418**, 244–251. (doi:10.1038/418244a)

Hassani, Z., Lemkine, G. F., Erbacher, P., Palmier, K., Alfama, G., Giovannangeli, C., Behr, J. P. & Demeneix, B. A. 2005 Lipid-mediated siRNA delivery down-regulates exogenous gene expression in the mouse brain at picomolar levels. *J. Gene Med.* **7**, 198–207. (doi:10.1002/jgm.659)

He, X. X., Chen, J. Y., Wang, K. M., Qin, D. L. & Tan, W. H. 2007 Preparation of luminescent Cy5 doped core-shell SFNPs and its application as a near-infrared fluorescent marker. *Talanta* **72**, 1519–1526. (doi:10.1016/j.talanta.2007.01.069)

Heer, S., Kompe, K., Gudel, H. U. & Haase, M. 2004 Highly efficient multicolour upconversion emission in transparent colloids of lanthanide-doped $NaYF_4$ nanocrystals. *Adv. Mater.* **16**, 2102–2105. (doi:10.1002/adma.200400772)

Hobbs, S. K., Monsky, W. L., Yuan, F., Roberts, W. G., Griffith, L., Torchilin, V. P. & Jain, R. K. 1998 Regulation of transport pathways in tumor vessels: role of tumor type and microenvironment. *Proc. Natl Acad. Sci. USA* **95**, 4607–4612. (doi:10.1073/pnas.95.8.4607)

Howard, K. A. *et al.* 2006 RNA interference *in vitro* and *in vivo* using a chitosan/siRNA nanoparticle system. *Mol. Ther.* **14**, 476–484. (doi:10.1016/j.ymthe.2006.04.010)

Huang, D. M. *et al.* 2005 Highly efficient cellular labeling of mesoporous nanoparticles in human mesenchymal stem cells: implication for stem cell tracking. *FASEB J.* **19**, 2014–2016.

Huang, C. K., Lo, C. L., Chen, H. H. & Hsiue, G. H. 2007 Multifunctional micelles for cancer cell targeting, distribution imaging, and anticancer drug delivery. *Adv. Funct. Mater.* **17**, 2291–2297. (doi:10.1002/adfm.200600818)

Hussain, S., Pluckthun, A., Allen, T. M. & Zangemeister-Wittke, U. 2007 Antitumor activity of an epithelial cell adhesion molecule-targeted nanovesicular drug delivery system. *Mol. Cancer Ther.* **6**, 3019–3027. (doi:10.1158/1535-7163.MCT-07-0615)

Iyer, G., Li, J. J., Pinaud, F., Tsay, J. M., Bentolila, L. A., Michalet, X. & Weiss, S. 2006. Near-infrared peptide-coated quantum dots for small animal imaging. In *Conf. on Colloidal Quantum Dots for Biomedical Applications, article 60960B*. San Jose, CA: Spie-International Society for Optical Engineering.

Jain, R. K. 2000 Delivery of molecular medicine to solid tumors: lessons from *in vivo* imaging of gene expression and function. In *Int. Symp. on Tumor Targeted Delivery Systems*. Bethesda, MD: Elsevier Science.

Jaiswal, J. K., Mattoussi, H., Mauro, J. M. & Simon, S. M. 2003 Long-term multiple color imaging of live cells using quantum dot bioconjugates. *Nat. Biotechnol.* **21**, 47–51. (doi:10.1038/nbt767)

Jaiswal, J. K., Goldman, E. R., Mattoussi, H. & Simon, S. M. 2004 Use of quantum dots for live cell imaging. *Nat. Methods* **1**, 73–78. (doi:10.1038/nmeth1004-73)

Jalil, R. A. & Zhang, Y. 2008 Biocompatibility of silica coated $NaYF_4$ upconversion fluorescent nanocrystals. *Biomaterials* **29**, 4122–4128. (doi:10.1016/j.biomaterials.2008.07.012)

Jiang, S. & Zhang, Y. 2008. IR-to-visible upconversion nanoparticles for *in vitro* fluorescent imaging. In *4th Kuala Lumpur International Conf. on Biomedical Engineering*. Kuala Lumpur, Malaysia: Springer.

Jiang, S., Zhang, Y., Lim, K. M., Sim, E. K. W. & Ye, L. 2009 NIR-to-visible upconversion nanoparticles for fluorescent labeling and targeted delivery of siRNA. *Nanotechnology* **20**, 155 101. (doi:10.1088/0957-4484/20/15/155101)

Kim, S. & Bawendi, M. G. 2003 Oligomeric ligands for luminescent and stable nanocrystal quantum dots. *J. Am. Chem. Soc.* **125**, 14 652–14 653. (doi:10.1021/ja0368094)

Kim, S. *et al.* 2004 Near-infrared fluorescent type II quantum dots for sentinel lymph node mapping. *Nat. Biotechnol.* **22**, 93–97. (doi:10.1038/nbt920)

Kim, D., Lee, E. S., Oh, K. T., Gao, Z. G. & Bae, Y. H. 2008*a* Doxorubicin-loaded polymeric micelle overcomes multidrug resistance of cancer by double-targeting folate receptor and early endosomal pH. *Small* **4**, 2043–2050. (doi:10.1002/smll.200701275)

Kim, J., Kim, H. S., Lee, N., Kim, T., Kim, H., Yu, T., Song, I. C., Moon, W. K. & Hyeon, T. 2008*b* Multifunctional uniform nanoparticles composed of a magnetite nanocrystal core and a mesoporous silica shell for magnetic resonance and fluorescence imaging and for drug delivery. *Angew. Chem. Int. Ed.* **47**, 8438–8441. (doi:10.1002/anie.200802469)

Kim, J., Lee, J. E., Lee, S. H., Yu, J. H., Lee, J. H., Park, T. G. & Hyeon, T. 2008*c* Designed fabrication of a multifunctional polymer nanomedical platform for simultaneous cancer-targeted imaging and magnetically guided drug delivery. *Adv. Mater.* **20**, 478–483. (doi:10.1002/adma.200701726)

Kim, J. H. *et al.* 2008*d* Antitumor efficacy of cisplatin-loaded glycol chitosan nanoparticles in tumor-bearing mice. *J. Control. Release* **127**, 41–49. (doi:10.1016/j.jconrel.2007.12.014)

Kirpotin, D. B., Drummond, D. C., Shao, Y., Shalaby, M. R., Hong, K. L., Nielsen, U. B., Marks, J. D., Benz, C. C. & Park, J. W. 2006 Antibody targeting of long-circulating lipidic nanoparticles does not increase tumor localization but does increase internalization in animal models. *Cancer Res.* **66**, 6732–6740. (doi:10.1158/0008-5472.CAN-05-4199)

Kuningas, K., Ukonaho, T., Pakkila, H., Rantanen, T., Rosenberg, J., Lovgren, T. & Soukka, T. 2006 Upconversion fluorescence resonance energy transfer in a homogeneous immunoassay for estradiol. *Anal. Chem.* **78**, 4690–4696. (doi:10.1021/ac0603983)

Kuningas, K., Pakkila, H., Ukonaho, T., Rantanen, T., Lovgren, T. & Soukka, T. 2007 Upconversion fluorescence enables homogeneous immunoassay in whole blood. *Clin. Chem.* **53**, 145–146. (doi:10.1373/clinchem.2006.076687)

Kurreck, J. 2009 RNA interference: from basic research to therapeutic applications. *Angew. Chem. Int. Ed.* **48**, 1378–1398. (doi:10.1002/anie.200802092)

Lagerholm, B. C., Wang, M. M., Ernst, L. A., Ly, D. H., Liu, H. J., Bruchez, M. P. & Waggoner, A. S. 2004 Multicolor coding of cells with cationic peptide coated quantum dots. *Nano Lett.* **4**, 2019–2022. (doi:10.1021/nl049295v)

Lai, C. Y., Trewyn, B. G., Jeftinija, D. M., Jeftinija, K., Xu, S., Jeftinija, S. & Lin, V. S. Y. 2003 A mesoporous silica nanosphere-based carrier system with chemically removable CdS nanoparticle caps for stimuli-responsive controlled release of neurotransmitters and drug molecules. *J. Am. Chem. Soc.* **125**, 4451–4459. (doi:10.1021/ja028650l)

Lakowicz, J. R., Gryczynski, I., Gryczynski, Z., Nowaczyk, K. & Murphy, C. J. 2000 Time-resolved spectral observations of cadmium-enriched cadmium sulfide nanoparticles and the effects of DNA oligomer binding. *Anal. Biochem.* **280**, 128–136. (doi:10.1006/abio.2000.4495)

Landen, C. N., Chavez-Reyes, A., Bucana, C., Schmandt, R., Deavers, M. T., Lopez-Berestein, G. & Sood, A. K. 2005 Therapeutic EphA2 gene targeting *in vivo* using neutral

liposomal small interfering RNA delivery. *Cancer Res.* **65**, 6910–6918. (doi:10.1158/0008-5472.CAN-05-0530)

Lee, H., Yu, M. K., Park, S., Moon, S., Min, J. J., Jeong, Y. Y., Kang, H. W. & Jon, S. 2007 Thermally cross-linked superparamagnetic iron oxide nanoparticles: synthesis and application as a dual imaging probe for cancer *in vivo*. *J. Am. Chem. Soc.* **129**, 12 739–12 745. (doi:10.1021/ja072210i)

Lee, C. H. *et al.* 2009 Near-infrared mesoporous silica nanoparticles for optical imaging: characterization and *in vivo* biodistribution. *Adv. Funct. Mater.* **19**, 215–222. (doi:10.1002/adfm.200800753)

Li, Z. Q. & Zhang, Y. 2006 Monodisperse silica-coated polyvinylpyrrolidone/$NaYF_4$ nanocrystals with multicolor upconversion fluorescence emission. *Angew. Chem. Int. Ed.* **45**, 7732–7735. (doi:10.1002/anie.200602975)

Li, Z. Q., Zhang, Y. & Jiang, S. 2008 Multicolor core/shell-structured upconversion fluorescent nanoparticles. *Adv. Mater.* **20**, 4765–4769. (doi:10.1002/adma.200801056)

Licha, K. & Olbrich, C. 2005 Optical imaging in drug discovery and diagnostic applications. *Adv. Drug Deliv. Rev.* **57**, 1087–1108. (doi:10.1016/j.addr.2005.01.021)

Lidke, D. S., Nagy, P., Heintzmann, R., Arndt-Jovin, D. J., Post, J. N., Grecco, H. E., Jares-Erijman, E. A. & Jovin, T. M. 2004 Quantum dot ligands provide new insights into erbB/HER receptor-mediated signal transduction. *Nat. Biotechnol.* **22**, 198–203. (doi:10.1038/nbt929)

Lieleg, O., Lopez-Garcia, M., Semmrich, C., Auernheimer, J., Kessler, H. & Bausch, A. R. 2007 Specific integrin labeling in living cells using functionalized nanocrystals. *Small* **3**, 1560–1565. (doi:10.1002/smll.200700148)

Lin, Y. S., Wu, S. H., Hung, Y., Chou, Y. H., Chang, C., Lin, M. L., Tsai, C. P. & Mou, C. Y. 2006 Multifunctional composite nanoparticles: magnetic, luminescent, and mesoporous. *Chem. Mater.* **18**, 5170–5172. (doi:10.1021/cm061976z)

Lisiecki, R., Ryba-Romanowski, W., Speghini, A. & Bettinelli, M. 2009 Luminescence spectroscopy of Er^{3+}-doped and Er^{3+}, Yb^{3+}-codoped $LaPO_4$ single crystals. *J. Lumin.* **129**, 521–525. (doi:10.1016/j.jlumin.2008.12.006)

Liu, Z. Y., Liu, M., Song, W. L., Pan, K., Li, J. H., Bai, Y. B. & Li, T. J. 2006 Multi-fluorescent dye-doped SiO_2/lanthanide complexes hybrid particles. *Mater. Lett.* **60**, 1629–1633. (doi:10.1016/j.matlet.2005.11.083)

Liu, Y. Y., Miyoshi, H. & Nakamura, M. 2007*a* Nanomedicine for drug delivery and imaging: a promising avenue for cancer therapy and diagnosis using targeted functional nanoparticles. *Int. J. Cancer* **120**, 2527–2537. (doi:10.1002/ijc.22709)

Liu, Z., Winters, M., Holodniy, M. & Dai, H. J. 2007*b* siRNA delivery into human T cells and primary cells with carbon-nanotube transporters. *Angew. Chem. Int. Ed.* **46**, 2023–2027. (doi:10.1002/anie.200604295)

Lovric, J., Bazzi, H. S., Cuie, Y., Fortin, G. R. A., Winnik, F. M. & Maysinger, D. 2005 Differences in subcellular distribution and toxicity of green and red emitting CdTe quantum dots. *J. Mol. Med.* **83**, 377–385. (doi:10.1007/s00109-004-0629-x)

Lu, J., Liong, M., Zink, J. I. & Tamanoi, F. 2007 Mesoporous silica nanoparticles as a delivery system for hydrophobic anticancer drugs. *Small* **3**, 1341–1346. (doi:10.1002/smll.200700005)

Martinez, J., Patkaniowska, A., Urlaub, H., Luhrmann, R. & Tuschl, T. 2002 Single-stranded antisense siRNAs guide target RNA cleavage in RNAi. *Cell* **110**, 563–574. (doi:10.1016/S0092-8674(02)00908-X)

Massoud, T. F. & Gambhir, S. S. 2003 Molecular imaging in living subjects: seeing fundamental biological processes in a new light. *Genes Dev.* **17**, 545–580. (doi:10.1101/gad.1047403)

Mattoussi, H., Mauro, J. M., Goldman, E. R., Green, T. M., Anderson, G. P., Sundar, V. C. & Bawendi, M. G. 2000. Bioconjugation of highly luminescent colloidal CdSe-ZnS quantum dots with an engineered two-domain recombinant protein. In *Int. Conf. on Semiconductor Quantum Dots* (*QD2000*). Munich, Germany: Wiley-VCH Verlag.

McCaffrey, A. P., Meuse, L., Pham, T. T. T., Conklin, D. S., Hannon, G. J. & Kay, M. A. 2002 Gene expression—RNA interference in adult mice. *Nature* **418**, 38–39. (doi:10.1038/418038a)

McNamara, J. O., Andrechek, E. R., Wang, Y., Viles, K. D., Rempel, R. E., Gilboa, E., Sullenger, B. A. & Giangrande, P. H. 2006 Cell type-specific delivery of siRNAs with aptamer–siRNA chimeras. *Nat. Biotechnol.* **24**, 1005–1015. (doi:10.1038/nbt1223)

Medarova, Z., Pham, W., Kim, Y., Dai, G. P. & Moore, A. 2006 *In vivo* imaging of tumor response to therapy using a dual-modality imaging strategy. *Int. J. Cancer* **118**, 2796–2802. (doi:10.1002/ijc.21672)

Medarova, Z., Pham, W., Farrar, C., Petkova, V. & Moore, A. 2007 *In vivo* imaging of siRNA delivery and silencing in tumors. *Nat. Med.* **13**, 372–377. (doi:10.1038/nm1486)

Medarova, Z., Rashkovetsky, L., Pantazopoulos, P. & Moore, A. 2009 Multiparametric monitoring of tumor response to chemotherapy by noninvasive imaging. *Cancer Res.* **69**, 1182–1189. (doi:10.1158/0008-5472.CAN-08-2001)

Miki, K., Kuramochi, Y., Oride, K., Inoue, S., Harada, H., Hiraoka, M. & Ohe, K. 2009 Ring-opening metathesis polymerization-based synthesis of ICG-containing amphiphilic triblock copolymers for *in vivo* tumor imaging. *Bioconjug. Chem.* **20**, 511–517. (doi:10.1021/bc800449s)

Moore, A., Medarova, Z., Potthast, A. & Dai, G. P. 2004 *In vivo* targeting of underglycosylated MUC-1 tumor antigen using a multimodal imaging probe. *Cancer Res.* **64**, 1821–1827. (doi:10.1158/0008-5472.CAN-03-3230)

Muratovska, A. & Eccles, M. R. 2004 Conjugate for efficient delivery of short interfering RNA (siRNA) into mammalian cells. *FEBS Lett.* **558**, 63–68. (doi:10.1016/S0014-5793(03)01505-9)

Nakanishi, T., Fukushima, S., Okamoto, K., Suzuki, M., Matsumura, Y., Yokoyama, M., Okano, T., Sakurai, Y. & Kataoka, K. 2000 Development of the polymer micelle carrier system for doxorubicin. In *Int. Symp. on Tumor Targeted Delivery Systems*. Bethesda, MD: Elsevier Science.

Nann, T. & Mulvaney, P. 2004 Single quantum dots in spherical silica particles. *Angew. Chem. Int. Ed.* **43**, 5393–5396. (doi:10.1002/anie.200460752)

Okuda, T., Kawakami, S., Akimoto, N., Niidome, T., Yamashita, F. & Hashida, M. 2006 PEGylated lysine dendrimers for tumor-selective targeting after intravenous injection in tumor-bearing mice. *J. Control. Release* **116**, 330–336. (doi:10.1016/j.jconrel.2006.09.012)

Parak, W. J. *et al.* 2002 Conjugation of DNA to silanized colloidal semiconductor nanocrystalline quantum dots. *Chem. Mater.* **14**, 2113–2119. (doi:10.1021/cm0107878)

Pathak, S., Choi, S.-K., Arnheim, N. & Thompson, M. E. 2001 Hydroxylated quantum dots as luminescent probes for in situ hybridization. *J. Am. Chem. Soc.* **123**, 4103–4104. (doi:10.1021/ja0058334)

Perk, L. R. *et al.* 2008 Quantitative PET imaging of Met-expressing human cancer xenografts with Zr-89-labelled monoclonal antibody DN30. *Eur. J. Nucl. Med. Mol. Imaging* **35**, 1857–1867. (doi:10.1007/s00259-008-0774-5)

Pirollo, K. F. & Chang, E. H. 2008 Does a targeting ligand influence nanoparticle tumor localization or uptake? *Trends Biotechnol.* **26**, 552–558. (doi:10.1016/j.tibtech.2008.06.007)

Qian, J. *et al.* 2007 Imaging pancreatic cancer using surface-functionalized quantum dots. *J. Phys. Chem. B* **111**, 6969–6972. (doi:10.1021/jp070620n)

Qian, H. S., Li, Z. Q. & Zhang, Y. 2008*a*. A facile synthesis of multicolor polystyrene microspheres encapsulating upconversion fluorescent nanoparticles. In *4th Kuala Lumpur Int. Conf. on Biomedical Engineering*. Kuala Lumpur, Malaysia: Springer.

Qian, J., Li, X., Wei, M., Gao, X. W., Xu, Z. P. & He, S. L. 2008*b* Bio-molecule-conjugated fluorescent organically modified silica nanoparticles as optical probes for cancer cell imaging. *Opt. Express* **16**, 19 568–19 578. (doi:10.1364/OE.16.019568)

Rana, T. M. 2007 Illuminating the silence: understanding the structure and function of small RNAs. *Nat. Rev. Mol. Cell Biol.* **8**, 23–36. (doi:10.1038/nrm2085)

Rao, J. H., Dragulescu-Andrasi, A. & Yao, H. Q. 2007 Fluorescence imaging *in vivo*: recent advances. *Curr. Opin. Biotechnol.* **18**, 17–25. (doi:10.1016/j.copbio.2007.01.003)

Reiss, P., Bleuse, J. & Pron, A. 2002 Highly luminescent CdSe/ZnSe core/shell nanocrystals of low size dispersion. *Nano Lett.* **2**, 781–784. (doi:10.1021/nl025596y)

Riehemann, K., Schneider, S. W., Luger, T. A., Godin, B., Ferrari, M. & Fuchs, H. 2009 Nanomedicine—challenge and perspectives. *Angew. Chem. Int. Ed.* **48**, 872–897. (doi:10.1002/anie.200802585)

Ross, J. S. & Fletcher, J. A. 1999 The HER-2/neu oncogene: prognostic factor, predictive factor and target for therapy. *Semin. Cancer Biol.* **9**, 125–138. (doi:10.1006/scbi.1998.0083)

Ruan, G., Agrawal, A., Marcus, A. I. & Nie, S. 2007 Imaging and tracking of tat peptide-conjugated quantum dots in living cells: new insights into nanoparticle uptake, intracellular transport, and vesicle shedding. *J. Am. Chem. Soc.* **129**, 14 759–14 766. (doi:10.1021/ja074936k)

Santra, S., Zhang, P., Wang, K. M., Tapec, R. & Tan, W. H. 2001 Conjugation of biomolecules with luminophore-doped silica nanoparticles for photostable biomarkers. *Anal. Chem.* **73**, 4988–4993. (doi:10.1021/ac010406+)

Santra, S., Dutta, D., Walter, G. A. & Moudgil, B. M. 2005 Fluorescent nanoparticle probes for cancer imaging. *Technol. Cancer Res. Treat.* **4**, 593–602.

Sanvicens, N. & Marco, M. P. 2008 Multifunctional nanoparticles—properties and prospects for their use in human medicine. *Trends Biotechnol.* **26**, 425–433. (doi:10.1016/j.tibtech.2008.04.005)

Satchi-Fainaro, R., Puder, M., Davies, J. W., Tran, H. T., Sampson, D. A., Greene, A. K., Corfas, G. & Folkman, J. 2004 Targeting angiogenesis with a conjugate of HPMA copolymer and TNP-470. *Nat. Med.* **10**, 255–261. (doi:10.1038/nm1002)

Schafer, H., Ptacek, P., Kompe, K. & Haase, M. 2007 Lanthanide-doped $NaYF_4$ nanocrystals in aqueous solution displaying strong up-conversion emission. *Chem. Mater.* **19**, 1396–1400. (doi:10.1021/cm062385b)

Selvan, S. T., Patra, P. K., Ang, C. Y. & Ying, J. Y. 2007 Synthesis of silica-coated semiconductor and magnetic quantum dots and their use in the imaging of live cells. *Angew. Chem. Int. Ed.* **46**, 2448–2452. (doi:10.1002/anie.200604245)

Shah, N., Cerussi, A., Eker, C., Espinoza, J., Butler, J., Fishkin, J., Hornung, R. & Tromberg, B. 2001 Noninvasive functional optical spectroscopy of human breast tissue. *Proc. Natl Acad. Sci. USA* **98**, 4420–4425. (doi:10.1073/pnas.071511098)

Shah, K., Jacobs, A., Breakefield, X. O. & Weissleder, R. 2004 Molecular imaging of gene therapy for cancer. *Gene Ther.* **11**, 1175–1187. (doi:10.1038/sj.gt.3302278)

Shi, D. L., Guo, Y., Dong, Z. Y., Lian, J., Wang, W., Liu, G. K., Wang, L. M. & Ewing, R. C. 2007*a* Quantum-dot-activated luminescent carbon nanotubes via a nano scale surface functionalization for *in vivo* imaging. *Adv. Mater.* **19**, 4033–4037. (doi:10.1002/adma.200700035)

Shi, H., He, X. X., Wang, K. M., Yuan, Y., Deng, K., Chen, J. Y. & Tan, W. H. 2007*b* Rhodamine B isothiocyanate doped silica-coated fluorescent nanoparticles (RBITC-DSFNPs)-based bioprobes conjugated to Annexin V for apoptosis detection and imaging. *Nanomed. Nanotechnol. Biol. Med.* **3**, 266–272. (doi:10.1016/j.nano.2007.08.004)

Shi, J. Y., Jia, B., Liu, Z. F., Yang, Z., Yu, Z. L., Chen, K., Chen, X. Y., Liu, S. & Wang, F. 2008 Tc-99m-labeled bombesin(7-14)NH_2 with favorable properties for SPECT imaging of colon cancer. *Bioconjug. Chem.* **19**, 1170–1178. (doi:10.1021/bc700471z)

Shiohara, A., Hoshino, A., Hanaki, K., Suzuki, K. & Yamamoto, K. 2004 On the cyto-toxicity caused by quantum dots. *Microbiol. Immunol.* **48**, 669–675.

Simberg, D. *et al.* 2007 Biomimetic amplification of nanoparticle homing to tumors. *Proc. Natl Acad. Sci. USA* **104**, 932–936. (doi:10.1073/pnas.0610298104)

Sinha, R., Kim, G. J., Nie, S. M. & Shin, D. M. 2006 Nanotechnology in cancer therapeutics: bioconjugated nanoparticles for drug delivery. *Mol. Cancer Ther.* **5**, 1909–1917. (doi:10.1158/1535-7163.MCT-06-0141)

Slamon, D. J. *et al.* 1989 Studies of the Her-2/Neu proto-oncogene in human-breast and ovarian-cancer. *Science* **244**, 707–712. (doi:10.1126/science.2470152)

Slowing, I. I., Trewyn, B. G., Giri, S. & Lin, V. S. Y. 2007 Mesoporous silica nanoparticles for drug delivery and biosensing applications. *Adv. Funct. Mater.* **17**, 1225–1236. (doi:10.1002/adfm.200601191)

Smith, B. R., Cheng, Z., De, A., Koh, A. L., Sinclair, R. & Gambhir, S. S. 2008 Real-time intravital imaging of RGD-quantum dot binding to luminal endothelium in mouse tumor neovasculature. *Nano Lett.* **8**, 2599–2606. (doi:10.1021/nl080141f)

Soltesz, E. G. *et al.* 2004. Intraoperative sentinel lymph node mapping of the lung using near-infrared fluorescent quantum dots. In *40th Annual Meeting of the Society of Thoracic Surgeons*. San Antonio, TX: Elsevier Science Inc.

Song, E. W. *et al.* 2005 Antibody mediated *in vivo* delivery of small interfering RNAs via cell-surface receptors. *Nat. Biotechnol.* **23**, 709–717. (doi:10.1038/nbt1101)

Sonoke, S., Ueda, T., Fujiwara, K., Sato, Y., Takagaki, K., Hirabayashi, K., Ohgi, T. & Yano, J. 2008 Tumor regression in mice by delivery of Bcl-2 small interfering RNA with pegylated cationic liposomes. *Cancer Res.* **68**, 8843–8851. (doi:10.1158/0008-5472.CAN-08-0127)

Soutschek, J. *et al.* 2004 Therapeutic silencing of an endogenous gene by systemic administration of modified siRNAs. *Nature* **432**, 173–178. (doi:10.1038/nature03121)

Suh, W. H., Suh, Y. H. & Stucky, G. D. 2009 Multifunctional nanosystems at the interface of physical and life sciences. *Nano Today* **4**, 27–36. (doi:10.1016/j.nantod.2008.10.013)

Sundaresan, G. *et al.* 2003 I-124-labeled engineered Anti-CEA minibodies and diabodies allow high-contrast, antigen-specific small-animal PET imaging of xenografts in athymic mice. *J. Nucl. Med.* **44**, 1962–1969.

Suyver, J. F., Grimm, J., Kramer, K. W. & Gudel, H. U. 2005 Highly efficient near-infrared to visible up-conversion process in $NaYF_4$:Er^{3+},Yb^{3+}. *J. Lumin.* **114**, 53–59. (doi:10.1016/j.jlumin.2004.11.012)

Suyver, J. F., Grimm, J., van Veen, M. K., Biner, D., Kramer, K. W. & Gudel, H. U. 2006 Upconversion spectroscopy and properties of $NaYF_4$ doped with Er^{3+}, Tm^{3+} and/or Yb^{3+}. *J. Lumin.* **117**, 1–12. (doi:10.1016/j.jlumin.2005.03.011)

Suzuki, H., Lee, I. Y. S. & Maeda, N. 2008 Laser-induced emission from dye-doped nanoparticle aggregates of poly (DL-lactide-co-glycolide). *Int. J. Phys. Sci.* **3**, 42–44.

Takeshita, F. *et al.* 2005 Efficient delivery of small interfering RNA to bone-metastatic tumors by using atelocollagen *in vivo*. *Proc. Natl Acad. Sci. USA* **102**, 12 177–12 182. (doi:10.1073/pnas.0501753102)

Talapin, D. V., Rogach, A. L., Kornowski, A., Haase, M. & Weller, H. 2001 Highly luminescent monodisperse CdSe and CdSe/ZnS nanocrystals synthesized in a hexadecylamine–trioctylphosphine oxide–trioctylphospine mixture. *Nano Lett.* **1**, 207–211. (doi:10.1021/nl0155126)

Tan, W. B., Jiang, S. & Zhang, Y. 2007 Quantum-dot based nanoparticles for targeted silencing of *HER2/neu* gene via RNA interference. *Biomaterials* **28**, 1565–1571. (doi:10.1016/j.biomaterials.2006.11.018)

Tanisaka, H., Kizaka-Kondoh, S., Makino, A., Tanaka, S., Hiraoka, M. & Kimura, S. 2008 Near-infrared fluorescent labeled peptosome for application to cancer imaging. *Bioconjug. Chem.* **19**, 109–117. (doi:10.1021/bc7001665)

Tapec, R., Zhao, X. J. J. & Tan, W. H. 2002 Development of organic dye-doped silica nanoparticles for bioanalysis and biosensors. *J. Nanosci. Nanotechnol.* **2**, 405–409. (doi:10.1166/jnn.2002.114)

Torchilin, V. P. 2006 Multifunctional nanocarriers. *Adv. Drug Deliv. Rev.* **58**, 1532–1555. (doi:10.1016/j.addr.2006.09.009)

Ukonaho, T., Rantanen, T., Jamsen, L., Kuningas, K., Pakkila, H., Lovgren, T. & Soukka, T. 2007 Comparison of infrared-excited up-converting phosphors and europium nanoparticles as labels in a two-site immunoassay. *Anal. Chim. Acta* **596**, 106–115. (doi:10.1016/j.aca.2007.05.060)

Ulbrich, K., Etrych, T., Chytil, P., Jelinkova, M. & Rihova, B. 2004 Antibody-targeted polymer-doxorubicin conjugates with pH-controlled activation. *J. Drug Target.* **12**, 477–489. (doi:10.1080/10611860400011869)

Ungun, B., Prud'homme, R. K., Budijono, S. J., Shan, J. N., Lim, S. F., Ju, Y. G. & Austin, R. 2009 Nanofabricated upconversion nanoparticles for photodynamic therapy. *Opt. Express* **17**, 80–86. (doi:10.1364/OE.17.000080)

Urban-Klein, B., Werth, S., Abuharbeid, S., Czubayko, F. & Aigner, A. 2005 RNAi-mediated gene-targeting through systemic application of polyethylenimine (PEI)-complexed siRNA *in vivo*. *Gene Ther.* **12**, 461–466. (doi:10.1038/sj.gt.3302425)

van de Rijke, F., Zijlmans, H., Li, S., Vail, T., Raap, A. K., Niedbala, R. S. & Tanke, H. J. 2001 Up-converting phosphor reporters for nucleic acid microarrays. *Nat. Biotechnol.* **19**, 273–276. (doi:10.1038/85734)

Villares, G. J. *et al.* 2008 Targeting melanoma growth and metastasis with systemic delivery of liposome-incorporated protease-activated receptor-1 small interfering RNA. *Cancer Res.* **68**, 9078–9086. (doi:10.1158/0008-5472.CAN-08-2397)

Vogel, A. & Venugopalan, V. 2003 Mechanisms of pulsed laser ablation of biological tissues. *Chem. Rev.* **103**, 577–644. (doi:10.1021/cr010379n)

Wang, L. Y. & Li, Y. D. 2006 Green upconversion nanocrystals for DNA detection. *Chem. Commun.* 2557–2559. (doi:10.1039/b604871d)

Wang, L., Yang, C. Y. & Tan, W. H. 2005*a* Dual-luminophore-doped silica nanoparticles for multiplexed signaling. *Nano Lett.* **5**, 37–43. (doi:10.1021/nl048417g)

Wang, L. Y., Yan, R. X., Hao, Z. Y., Wang, L., Zeng, J. H., Bao, H., Wang, X., Peng, Q. & Li, Y. D. 2005*b* Fluorescence resonant energy transfer biosensor based on upconversion-luminescent nanoparticles. *Angew. Chem. Int. Ed.* **44**, 6054–6057. (doi:10.1002/anie.200501907)

Wang, F., Chatterjee, D. K., Li, Z. Q., Zhang, Y., Fan, X. P. & Wang, M. Q. 2006 Synthesis of polyethylenimine/$NaYF_4$ nanoparticles with upconversion fluorescence. *Nanotechnology* **17**, 5786–5791. (doi:10.1088/0957-4484/17/23/013)

Wang, X., Yang, L. L., Chen, Z. & Shin, D. M. 2008 Application of nanotechnology in cancer therapy and imaging. *CA, Cancer J. Clin.* **58**, 97–110. (doi:10.3322/CA.2007.0003)

Wartlick, H., Michaelis, K., Balthasar, S., Strebhardt, K., Kreuter, J. & Langer, K. 2004 Highly specific HER2-mediated cellular uptake of antibody-modified nanoparticles in tumour cells. *J. Drug Target.* **12**, 461–471. (doi:10.1080/10611860400010697)

Weissleder, R. 2006 Molecular imaging in cancer. *Science* **312**, 1168–1171. (doi:10.1126/science.1125949)

Weng, K. C. *et al.* 2008 Targeted tumor cell internalization and imaging of multifunctional quantum dot-conjugated immunoliposomes *in vitro* and *in vivo*. *Nano Lett.* **8**, 2851–2857. (doi:10.1021/nl801488u)

Winter, J. O., Liu, T. Y., Korgel, B. A. & Schmidt, C. E. 2001 Recognition molecule directed interfacing between semiconductor quantum dots and nerve cells. *Adv. Mater.* **13**, 1673–1677. (doi:10.1002/1521-4095(200111)13:22<1673::AID-ADMA1673>3.0.CO;2-6)

Wu, A. M. *et al.* 2000 High-resolution microPET imaging of carcino-embryonic antigen-positive xenografts by using a copper-64-labeled engineered antibody fragment. *Proc. Natl Acad. Sci. USA* **97**, 8495–8500. (doi:10.1073/pnas.150228297)

Wu, X. Y., Liu, H. J., Liu, J. Q., Haley, K. N., Treadway, J. A., Larson, J. P., Ge, N. F., Peale, F. & Bruchez, M. P. 2003 Immunofluorescent labeling of cancer marker Her2 and other cellular targets with semiconductor quantum dots. *Nat. Biotechnol.* **21**, 41–46. (doi:10.1038/nbt764)

Wu, S. H., Lin, Y. S., Hung, Y., Chou, Y. H., Hsu, Y. H., Chang, C. & Mou, C. Y. 2008 Multifunctional mesoporous silica nanoparticles for intracellular labeling and animal magnetic resonance imaging studies. *Chembiochem* **9**, 53–57. (doi:10.1002/cbic.200700509)

Xing, Y. & Rao, J. H. 2008 Quantum dot bioconjugates for *in vitro* diagnostics & *in vivo* imaging. *Cancer Biomarkers* **4**, 307–319.

Xing, Y. *et al.* 2007 Bioconjugated quantum dots for multiplexed and quantitative immunohistochemistry. *Nat. Protoc.* **2**, 1152–1165. (doi:10.1038/nprot.2007.107)

Xiong, X. B., Uludag, H. & Lavasanifar, A. 2009 Biodegradable amphiphilic poly(ethylene oxide)-block-polyesters with grafted polyamines as supramolecular nanocarriers for efficient siRNA delivery. *Biomaterials* **30**, 242–253. (doi:10.1016/j.biomaterials.2008.09.025)

Xu, Z. H., Gu, W. W., Huang, J., Sui, H., Zhou, Z. H., Yang, Y. X., Yan, Z. & Li, Y. P. 2005 In vitro and in vivo evaluation of actively targetable nanoparticles for paclitaxel delivery. *Int. J. Pharm.* **288**, 361–368. (doi:10.1016/j.ijpharm.2004.10.009)

Yang, Z., Zheng, S. Y., Harrison, W. J., Harder, J., Wen, X. X., Gelovani, J. G., Qiao, A. & Li, C. 2007 Long-circulating near-infrared fluorescence core-cross-linked polymeric micelles: synthesis, characterization, and dual nuclear/optical imaging. *Biomacromolecules* **8**, 3422–3428. (doi:10.1021/bm7005399)

Yezhelyev, M. V. *et al.* 2007 *In situ* molecular profiling of breast cancer biomarkers with multicolor quantum dots. *Adv. Mater.* **19**, 3146–3151. (doi:10.1002/adma.200701983)

Yezhelyev, M. V., Qi, L. F., O'Regan, R. M., Nie, S. & Gao, X. H. 2008 Proton-sponge coated quantum dots for

siRNA delivery and intracellular imaging. *J. Am. Chem. Soc.* **130**, 9006–9012. (doi:10.1021/ja800086u)

Yi, D. K., Selvan, S. T., Lee, S. S., Papaefthymiou, G. C., Kundaliya, D. & Ying, J. Y. 2005 Silica-coated nanocomposites of magnetic nanoparticles and quantum dots. *J. Am. Chem. Soc.* **127**, 4990–4991. (doi:10.1021/ja0428863)

Yong, K. T. 2009 Mn-doped near-infrared quantum dots as multimodal targeted probes for pancreatic cancer imaging. *Nanotechnology* **20**, 015 102. (doi:10.1088/0957-4484/20/1/015102)

Zhang, Y. & Huang, N. 2006 Intracellular uptake of CdSe-ZnS/polystyrene nanobeads. *J. Biomed. Mater. Res. Part B Appl. Biomater.* **76B**, 161–168. (doi:10.1002/jbm.b.30347)

Zhou, X. C. & Zhou, J. Z. 2004 Improving the signal sensitivity and photostability of DNA hybridizations on microarrays by using dye-doped core-shell silica nanoparticles. *Anal. Chem.* **76**, 5302–5312. (doi:10.1021/ac049472c)

Zijlmans, H., Bonnet, J., Burton, J., Kardos, K., Vail, T., Niedbala, R. S. & Tanke, H. J. 1999 Detection of cell and tissue surface antigens using up-converting phosphors: a new reporter technology. *Anal. Biochem.* **267**, 30–36. (doi:10.1006/abio.1998.2965)

Zimmer, J. P., Kim, S. W., Ohnishi, S., Tanaka, E., Frangioni, J. V. & Bawendi, M. G. 2006 Size series of small indium arsenide-zinc selenide core-shell nanocrystals and their application to *in vivo* imaging. *J. Am. Chem. Soc.* **128**, 2526–2527. (doi:10.1021/ja0579816)